



## Simulation of evapotranspiration and yield of maize

Bruce Kimball, Kelly Thorp, Kenneth Boote, Claudio Stockle, Andrew Suyker, Steven Evett, David Brauer, Gwen Coyle, Karen Copeland, Gary Marek, et al.

### ► To cite this version:

Bruce Kimball, Kelly Thorp, Kenneth Boote, Claudio Stockle, Andrew Suyker, et al.. Simulation of evapotranspiration and yield of maize. *Agricultural and Forest Meteorology*, 2023, 333, pp.109396. 10.1016/j.agrformet.2023.109396 . hal-04112537

**HAL Id: hal-04112537**

**<https://hal.inrae.fr/hal-04112537v1>**

Submitted on 28 Aug 2023

**HAL** is a multi-disciplinary open access archive for the deposit and dissemination of scientific research documents, whether they are published or not. The documents may come from teaching and research institutions in France or abroad, or from public or private research centers.

L'archive ouverte pluridisciplinaire **HAL**, est destinée au dépôt et à la diffusion de documents scientifiques de niveau recherche, publiés ou non, émanant des établissements d'enseignement et de recherche français ou étrangers, des laboratoires publics ou privés.



Distributed under a Creative Commons Attribution - NonCommercial - NoDerivatives 4.0 International License

# Simulation of Evapotranspiration and Yield of Maize: An Inter-comparison among 41 Maize Models

By

**Bruce A. Kimball<sup>1</sup>, Kelly R. Thorp<sup>1</sup>, Kenneth J. Boote<sup>2</sup>, Claudio Stockle<sup>3</sup>, Andrew E. Suyker<sup>4</sup>, Steven R. Evett<sup>5</sup>, David K. Brauer<sup>5</sup>, Gwen G. Coyle<sup>5</sup>, Karen S. Copeland<sup>5</sup>, Gary W. Marek<sup>5</sup>, Paul D. Colaizzi<sup>5</sup>, Marco Acutis<sup>6</sup> Seyyedmajid Alimaghani<sup>7</sup>, Sotirios Archontoulis<sup>8</sup>, Faye Babacar<sup>9</sup>, Zoltán Barcza<sup>10,11</sup>, Bruno Basso<sup>12</sup>, Patrick Bertuzzi<sup>13</sup>, Julie Constantin<sup>14</sup>, Massimiliano De Antoni Migliorati<sup>15</sup>, Benjamin Dumont<sup>16</sup>, Jean-Louis Durand<sup>17</sup>, Nándor Fodor<sup>11,18</sup>, Thomas Gaiser<sup>19</sup>, Pasquale Garofalo<sup>20</sup>, Sebastian Gayler<sup>21</sup>, Luisa Giglio<sup>20</sup>, Robert Grant<sup>22</sup>, Kaiyu Guan<sup>23</sup>, Gerrit Hoogenboom<sup>2</sup>, Qianjing Jiang<sup>24</sup>, Soohyung Kim<sup>25</sup>, Isaya Kisekka<sup>26</sup>, Jon Lizaso<sup>27</sup>, Sara Masia<sup>28</sup>, Huimin Meng<sup>29</sup>, Valentina Mereu<sup>30</sup>, Ahmed Mukhtar<sup>31</sup>, Alessia Perego<sup>6</sup>, Bin Peng<sup>23</sup>, Eckart Priesack<sup>32</sup>, Zhiming Qi<sup>24</sup>, Vakhtang Shelia<sup>2</sup>, Richard Snyder<sup>33</sup>, Afshin Soltani<sup>7</sup>, Donatella Spano<sup>30</sup>, Amit Srivastava<sup>19</sup>, Aimee Thomson<sup>34</sup>, Dennis Timlin<sup>35</sup>, Antonio Trabucco<sup>30</sup>, Heidi Webber<sup>36</sup>, Tobias Weber<sup>21</sup>, Magali Willaume<sup>14</sup>, Karina Williams<sup>37,38</sup>, Michael van der Laan<sup>34</sup>, Domenico Ventrella<sup>20</sup>, Michelle Viswanathan<sup>21</sup>, Xu Xu<sup>29</sup>, Wang Zhou<sup>23</sup>**

<sup>1</sup>U.S. Arid-Land Agricultural Research Center, USDA-ARS, Maricopa, AZ 85138

([bruce.kimball@usda.gov](mailto:bruce.kimball@usda.gov); [kelly.thorp@usda.gov](mailto:kelly.thorp@usda.gov))

<sup>2</sup>University of Florida, Agricultural and Biological Engineering, Frazier Rogers Hall,

Gainesville, Florida 32611-0570, USA ([kjboote@ufl.edu](mailto:kjboote@ufl.edu); [gerrit@ufl.edu](mailto:gerrit@ufl.edu);

[vakhtang.shelia@ufl.edu](mailto:vakhtang.shelia@ufl.edu))

<sup>3</sup>Biological Systems Engineering, Washington State University, 1935 E. Grimes Way, PO Box

646120, Washington State University, Pullman WA 99164-6120 ([stockle@wsu.edu](mailto:stockle@wsu.edu))

<sup>4</sup>School of Natural Resources, University of Nebraska-Lincoln, Lincoln, Nebraska, USA

([asuyker1@unl.edu](mailto:asuyker1@unl.edu))

<sup>5</sup>Conservation and Production Research Laboratory, USDA-ARS, Bushland, Texas, USA

([Steve.Evett@usda.gov](mailto:Steve.Evett@usda.gov); [david.brauer@usda.gov](mailto:david.brauer@usda.gov); [gwen.coyle@usda.gov](mailto:gwen.coyle@usda.gov);

[karen.copeland@usda.gov](mailto:karen.copeland@usda.gov); [gary.marek@usda.gov](mailto:gary.marek@usda.gov); [paul.colaiizzi@usda.gov](mailto:paul.colaiizzi@usda.gov))

<sup>6</sup>Department of Agricultural and Environmental Sciences, University of Milan, via Celoria 2 –

20133, Milan, Italy ([marco.acutis@unimi.it](mailto:marco.acutis@unimi.it), [alessia.perego@unimi.it](mailto:alessia.perego@unimi.it))

32

33 <sup>7</sup>Agronomy Group, Gorgan Univ. of Agric. Sci. & Natur. Resour., Gorgan 49138-15739 Iran  
34 ([Afshin.Soltani@gmail.com](mailto:Afshin.Soltani@gmail.com); [m.alimagham@gmail.com](mailto:m.alimagham@gmail.com))

35 <sup>8</sup>Iowa State University, Department of Agronomy, Ames, Iowa 50010 ([sarchont@iastate.edu](mailto:sarchont@iastate.edu); 1-  
36 515-294-7413)

37 <sup>9</sup>Institut de recherche pour le développement (IRD) ESPACE-DEV, F-34093 Montpellier Cedex,  
38 France ([babacar.faye@ird.fr](mailto:babacar.faye@ird.fr))

39 <sup>10</sup>ELTE Eötvös Loránd University, Department of Meteorology, H-1192 Budapest, Hungary  
40 ([zoltan.barcza@ttk.elte.hu](mailto:zoltan.barcza@ttk.elte.hu))

41  
42 <sup>11</sup>Czech University of Life Sciences Prague, Faculty of Forestry and Wood Sciences, 165 21  
43 Prague, Czech Republic

44 <sup>12</sup>Michigan State University, Dept. Geological Sciences and W.K. Kellogg Biological Station,  
45 288 Farm Ln, 307 Natural Science Bldg., East Lansing, MI, 48824 ([basso@msu.edu](mailto:basso@msu.edu))

46 <sup>13</sup>US1116 AgroClim, INRAE centre de recherche Provence-Alpes-Côte d'Azur, 228, route de  
47 l'Aérodrome, CS 40 509, Domaine Saint Paul, Site Agroparc, 84914 Avignon Cedex 9, France  
48 ([agroclim-contact@inrae.fr](mailto:agroclim-contact@inrae.fr))

49 <sup>14</sup>AGIR, Université de Toulouse, INRAE, INPT, INP- EI PURPAN, 24 Chemin de Borde Rouge  
50 - Auzeville CS 52627, CastanetTolosan, France ([julie.constantin@toulouse.inra.fr](mailto:julie.constantin@toulouse.inra.fr);  
51 [magali.willaume@ensat.fr](mailto:magali.willaume@ensat.fr)).

52 <sup>15</sup>Queensland Department of Environment & Science, Queensland, Australia  
53 ([Max.DeAntoni@des.qld.gov.au](mailto:Max.DeAntoni@des.qld.gov.au))

54 <sup>16</sup>ULiege-GxABT, University of Liege - Gembloux Agro-Bio Tech, TERRA Teaching and  
55 research centre, Plant Science Axis / Crop Science Lab., B-5030 Gembloux, Belgium  
56 ([Benjamin.Dumont@uliege.be](mailto:Benjamin.Dumont@uliege.be))

57 <sup>17</sup>Unité de Recherches Pluridisciplinaire Prairies et Plantes Fourragères, INRAE, 86 600  
58 Lusignan, France ([jean-louis.durand@inra.fr](mailto:jean-louis.durand@inra.fr))

59 <sup>18</sup>Agricultural Institute, Centre for Agricultural Research, H-2462 Martonvásár, Brunszvik u. 2.,  
60 Hungary ([fodor.nandor@atk.hu](mailto:fodor.nandor@atk.hu))

61 <sup>19</sup>Institute of Crop Science and Resource Conservation, University of Bonn, Katzenburgweg 5  
62 D-53115 Bonn, Germany ([tgaiser@uni-bonn.de](mailto:tgaiser@uni-bonn.de); [amit.srivastava@uni-bonn.de](mailto:amit.srivastava@uni-bonn.de))

63 <sup>20</sup>Council for Agricultural Research and Economics, Agriculture and Environment Research  
64 Center, CREA-AA, Via Celso Ulpiani 5, 70125 BARI BA, Italy ([pasquale.garofalo@crea.gov.it](mailto:pasquale.garofalo@crea.gov.it);  
65 [luisa.giglio@crea.gov.it](mailto:luisa.giglio@crea.gov.it); [domenico.ventrella@crea.gov.it](mailto:domenico.ventrella@crea.gov.it))

66 <sup>21</sup>Universität Hohenheim, Institute of Soil Science and Land Evaluation, Biogeophysics, Emil-  
67 Wolff-Str. 27, D-70593 Stuttgart, Germany ([sebastian.gayler@uni-hohenheim.de](mailto:sebastian.gayler@uni-hohenheim.de);  
68 [tobias.weber@uni-hohenheim.de](mailto:tobias.weber@uni-hohenheim.de); [michelle.viswanathan@uni-hohenheim.de](mailto:michelle.viswanathan@uni-hohenheim.de))

69 <sup>22</sup>Department of Renewable Resources, University of Alberta, Edmonton, Alberta, Canada T6G  
70 2E3 ([rgrant@ualberta.ca](mailto:rgrant@ualberta.ca))

71 <sup>23</sup>College of Agricultural, Consumer and Environmental Sciences (ACES), University of Illinois  
72 at Urbana-Champaign, Urbana, Illinois 61801, USA ([kaiyug@illinois.edu](mailto:kaiyug@illinois.edu);  
73 [binpeng@illinois.edu](mailto:binpeng@illinois.edu); [wangzhou@illinois.edu](mailto:wangzhou@illinois.edu))

74 <sup>24</sup>Department of Bioresource Engineering, Macdonald Campus, McGill University, 1-024  
75 Macdonald-Steward Hall, Sainte-Anne-de-Bellevue, QC, Canada H9X 3V9  
76 ([qianjing.jiang@mail.mcgill.ca](mailto:qianjing.jiang@mail.mcgill.ca); [zhiming.qi@mcgill.ca](mailto:zhiming.qi@mcgill.ca))

77 <sup>25</sup>School of Environmental and Forest Sciences, University of Washington, Seattle, WA 98195  
78 ([soohkim@uw.edu](mailto:soohkim@uw.edu))

79 <sup>26</sup>Agricultural Water Management and Irrigation Engineering; University of California Davis;  
80 Departments of Land, Air, and Water Resources and of Biological and Agricultural Engineering;  
81 One Shields Avenue; PES 1110; Davis, CA 95616-5270, USA ([ikisekka@ucdavis.edu](mailto:ikisekka@ucdavis.edu))

82 <sup>27</sup>Technical University of Madrid (UPM), Dept. Producción Agraria-CEIGRAM, Ciudad  
83 Universitaria, 28040 Madrid, Spain ([jon.lizaso@upm.es](mailto:jon.lizaso@upm.es))

84 <sup>28</sup>Land and Water Management Department, IHE Delft Institute for Water Education, Delft, The  
85 Netherlands ([sara.masia@cmcc.it](mailto:sara.masia@cmcc.it))

86 <sup>29</sup>Center of Agricultural Water Research, China Agricultural University, Beijing, China  
87 ([mhm2019@163.com](mailto:mhm2019@163.com); [xushengwu@cau.edu.cn](mailto:xushengwu@cau.edu.cn))

88 <sup>30</sup>Fondazione CMCC - Euro-Mediterranean Centre on Climate Change, Impacts on Agriculture,  
89 Forests and Ecosystem Services division (IAFES), Sassari, ITALY ([antonio.trabucco@cmcc.it](mailto:antonio.trabucco@cmcc.it);  
90 [spano@uniss.it](mailto:spano@uniss.it); [valentina.mereu@cmcc.it](mailto:valentina.mereu@cmcc.it))

91 <sup>31</sup>Department of Agronomy, PMAS Arid Agriculture University, Rawalpindi, Pakistan and  
92 Swedish University of Agricultural Sciences, Umea Sweden ([mukhtar.ahmed@slu.se](mailto:mukhtar.ahmed@slu.se))

93 <sup>32</sup>Helmholtz Center Munich, Institute of Biochemical Plant Pathology, Ingolstaedter Landstr. 1  
94 85764 Neuherberg, Germany ([priesack@helmholtz-muenchen.de](mailto:priesack@helmholtz-muenchen.de))

95 <sup>33</sup>University of California Davis ([rlsnyder@ucdavis.edu](mailto:rlsnyder@ucdavis.edu))

96 <sup>34</sup>University of Pretoria, Pretoria, South Africa ([michael.vanderlaan@up.ac.za](mailto:michael.vanderlaan@up.ac.za);  
97 [u16015925@tuks.co.za](mailto:u16015925@tuks.co.za))

98 <sup>35</sup>Crop Systems and Global Change Research Unit, USDA-ARS, Beltsville, MD  
99 ([Dennis.Timlin@ars.usda.gov](mailto:Dennis.Timlin@ars.usda.gov))

<sup>36</sup>Leibniz Centre for Agricultural Landscape Research (ZALF), Mucheberg 15374, Germany  
(webber@zalf.de)

<sup>37</sup>Hadley Centre, FitzRoy, Road Exeter Devon EX1 3PB, United Kingdom  
([karina.williams@metoffice.gov.uk](mailto:karina.williams@metoffice.gov.uk))

<sup>38</sup>Global Systems Institute, University of Exeter, North Park Road, Exeter, EX4 4QE, UK

Corresponding Author:

Bruce A. Kimball

U.S. Arid-Land Agricultural Research Center

USDA, Agricultural Research Service

21881 North Cardon Lane

Maricopa, Arizona 85018, USA

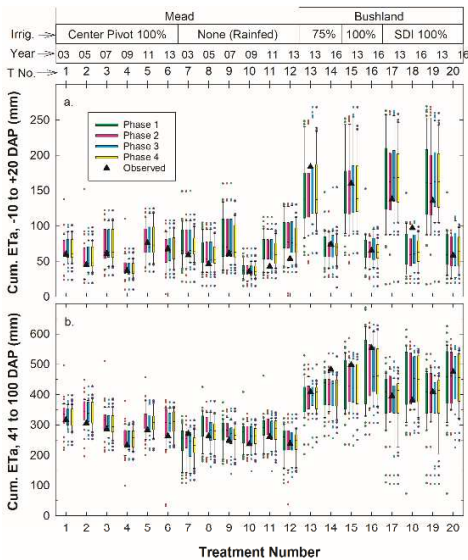
(phone: 1-602-840-4352; email: [bruce.kimball@usda.gov](mailto:bruce.kimball@usda.gov))

## **Abstract**

Accurate simulation of crop water use (evapotranspiration, ET) can help crop growth models to assess the likely effects of climate change on future crop productivity, as well as being an aid for irrigation scheduling for today's growers. To determine how well maize (*Zea mays* L.) growth models can simulate ET, an initial inter-comparison study was conducted in 2019 under the umbrella of AgMIP (Agricultural Model Inter-Comparison and Improvement Project). Herein, we present results of a second inter-comparison study of 41 maize models that was conducted using more comprehensive datasets from two additional sites - Mead, Nebraska, USA and

Bushland, Texas, USA. There were 20 treatment-years with varying irrigation levels over multiple seasons at both sites. ET was measured using eddy covariance at Mead and using large weighing lysimeters at Bushland. A wide range in ET rates was simulated among the models, yet several generally were able to simulate ET rates adequately. The ensemble median values were generally close to the observations, but a few of the models sometimes performed better than the median. Many of the models that did well at simulating ET for the Mead site did poorly for drier, windy days at the Bushland site, suggesting they need to improve how they handle humidity and wind. Additional variability came from the approaches used to simulate soil water evaporation. Fortunately, several models were identified that did well at simulating soil water evaporation, canopy transpiration, biomass accumulation, and grain yield. These models were older and have been widely used, which suggests that a larger number of users have tested these models over a wider range of conditions leading to their improvement. These revelations of the better approaches are leading to model improvements and more accurate simulations of ET.

### Graphical abstract



## Highlights

- Maize growth models differ widely in their simulations of daily evapotranspiration
- Most models fail to sufficiently reduce transpiration after crop maturation
- Most models fail to adequately reproduce effects of low humidity and high windspeed
- The median of models was often but not always the best performing
- Model inter-comparisons suggest avenues to improve simulation of maize ET

**Keywords:** Maize; simulation; evapotranspiration; water use; crop models; yield

## 1 Introduction

Crop growth models are a useful management aid for today's farmers, as well as being a tool to forecast the likely effects of climate change on future agricultural productivity and irrigation water requirements. For both tasks they need to be accurate. Therefore, in a major effort to improve their accuracy and reliability, modeling groups within the Agricultural Model Inter-comparison and Improvement Project (AgMIP; <https://agmip.org/>) have been inter-comparing multiple models against each other and against field datasets with varying CO<sub>2</sub>, temperature, nitrogen fertilizer, and water supply [wheat (*Triticum aestivum* L.; Asseng et al., 2013, 2015; Cammarano et al., 2016; Liu et al., 2016; Maiorano et al., 2017; Wang et al., 2017), maize (*Zea mays* L.; Bassu et al., 2014; Durand et al., 2018; Kimball et al., 2019), rice (*Oryza sativa* L.; Li

<sup>1</sup> Abbreviations: ASCE – American Society of Civil Engineers, DAP – days after planting, E – soil water evaporation, Ep – potential soil water evaporation, Es – simulated soil water evaporation, ET – evapotranspiration, ETo – “short” reference evapotranspiration based on 12-cm-tall grass, ETp – potential evapotranspiration, ETr – “tall” reference evapotranspiration based on 50-cm-tall alfalfa, ETs – simulated evapotranspiration, LAI, leaf area index, nRMSE – normalized root mean square error, MESA – mid-elevation sprinkler application, P-T – Priestley-Taylor, SDI – subsurface drip irrigation, T – transpiration, Tp – potential canopy transpiration, Ts – simulated canopy transpiration



et al., 2015; Hasegawa et al., 2017), and potato (*Solanum tuberosum* L.; Fleisher et al., 2017)].

As discussed by Kimball et al. (2019), only a few comparisons among methods or models to simulate ET have been done previously. Sau et al. (2004) evaluated several ET options with the CROPGRO Faba bean (*Vicia faba* L.) model, by careful comparison to soil water balance, and found that the FAO-56 option (Allen et al., 1998) had a root mean square error (RMSE) that was 20% smaller than the Priestley-Taylor option (Priestley and Taylor, 1972) and 48% smaller than the FAO-24 option (Doorenbos and Pruitt, 1985). In an inter-comparison of water use among wheat models at four sites around the world, Cammarano et al. (2016) found the coefficient of variation was only 22.5% among models and sites. In contrast, in an inter-comparison among maize models, Bassu et al. (2014) found a very large range of simulated values of ET among the models, including -10 to +30% variations in the ET response to doubled CO<sub>2</sub> concentration (720 µmol/mol). However, there were no observations of ET or water use in the dataset chosen for that study, so there was no standard for comparison. Therefore, Kimball et al. (2019) conducted their study using eight seasons of data from Ames, Iowa, USA for which eddy covariance measurements of ET were available. Like Bassu et al. (2014), they also found simulated ET values varied by a factor of two among the maize models. Surprisingly, among the models with closest agreement to observations, some were quite simple (e.g., no simulation of biomass) and some were quite complex (e.g., full energy balance), so it was difficult to determine which approaches were generally best and should be adopted by the poorer performing models. Nevertheless, there were several cases in which different ET methods were tested within the same family of crop models, and comparisons among these methods clearly revealed some approaches that were better than others.

However, there were some issues with the Ames dataset (Kimball et al., 2019). For example, in 2012, an infamous year for drought in the Midwest, observed ET and crop yield were higher than in other years. Further analysis led to the strong suspicion that there was a water table present to provide additional water besides the sparse rainfall, yet deep soil water measurements were lacking to confirm the suspicion. Therefore, it was decided to repeat the study of Kimball et al. (2019) with more robust datasets.

Two such datasets were identified, one from the University of Nebraska at Mead, Nebraska, USA (41.165°N, 96.470°W, 362 m), which is close to the 100<sup>th</sup> meridian typically used to divide the humid East from the arid West, thus placing it within the U.S. “corn belt.” There were six seasons of maize from irrigated and rainfed fields (12 treatment-years) with ET determined using eddy covariance. The second was collected by the USDA, Agricultural Research Service, Conservation and Production Research Laboratory (CPRL), Bushland, Texas, USA (35.183°N, 102.100°W, 1170 m), which is a more arid region where maize is mostly grown with irrigation, and where winds are commonly higher. They measured ET using large weighing lysimeters. They grew maize for two seasons with MESA (mid-elevation sprinkler application) at 100% and 75% replacement of soil water and in near-duplicate SDI (sub-surface drip irrigation) fields at 100% (8 treatment-years). A total of 41 models participated in this second round of maize ET simulation inter-comparisons (Tables 1, S1), and again the primary objective was to identify the approaches that were most accurate for simulating ET, i.e., had the lowest RMSE compared to the observations. Besides ET, other objectives were to test the models’ abilities to simulate LAI, biomass, grain yield, soil moisture, and soil temperature. By “approaches” we mean the methods

used by the models to simulate ET or other processes, i.e., FAO-56 (Allen et al. 1998) versus Priestley-Taylor (1972), etc.

## **2 Materials and Methods**

### *2.1 Observed data*

#### *2.1.1 University of Nebraska, Mead, Nebraska, USA*

One set of field data came from the University of Nebraska Agricultural Research and Development Center near Mead, Nebraska, USA (<http://csp.unl.edu/public/>). The soils were deep silty clay loams of Yutan (fine-silty, mixed, superactive, mesic Mollic Hapludalfs), Tomek (fine, smectitic, mesic Pachic Argialbolls), Filbert (fine, smectitic, mesic Vertic Argialbolls), and Filmore (fine, smectitic, mesic Vertic Argialbolls). The eddy covariance technique was used to determine ET of maize and soybean (*Glycine max*) in alternate years, as well as fluxes of sensible heat and CO<sub>2</sub>. Additional details can be found in Suyker and Verma (2008, 2009) and Suyker et al. (2004, 2005). Briefly, fluxes of latent heat, sensible heat, and momentum were determined using data from the following sensors at each site: an omnidirectional 3D sonic anemometer (Model R3: Gill Instruments Ltd., Lymington, UK) and an open-path infrared CO<sub>2</sub>/H<sub>2</sub>O gas analyzing system (Model LI7500: Li-Cor Inc., Lincoln, NE).

The instruments were deployed near the centers of the fields, and the fetch was about 400 m in all directions. The eddy covariance sensors were mounted 5.5 m above the ground. Fluxes were corrected for inadequate sensor frequency, and they were also adjusted for the variation in air density due to the transfer of water vapor and sensible heat. Air temperature and relative

humidity (Humitter50Y, Vaisala, Helsinki, FIN), soil heat flux at 0.06m (Radiation and Energy Balance Systems, Inc., Seattle, WA), and net radiation at 5.5m (CNR1, Kipp and Zonen Ltd., Delft, NLD) were also measured. Missing data due to sensor malfunction, power outages, unfavorable weather, etc. (approximately 15–20% per year), were estimated using an approach that combined measurement, interpolation, and empirical data synthesis. When hourly values were missing (day or night), the latent heat values were estimated as a function of available energy. Linear regressions between latent heat and available energy were determined (separately for dry and wet conditions) for sliding 3-day intervals, and these estimates were used to fill in missing flux values.

To check closure of the energy balance, the sum of latent and sensible heat fluxes ( $\lambda E + H$ ) measured by eddy covariance were plotted against the sum of  $R_n$  (net radiation) + four storage terms, determined by other methods (e.g., Suyker and Verma, 2008). Linear regressions were calculated between the hourly values of  $H + \lambda E$  and  $R_n + G$  at the study sites (excluding winter months and periods with rain and irrigation). Here  $G = G_s$  (soil heat storage) +  $G_c$  (canopy heat storage) +  $G_m$  (heat stored in the mulch) +  $G_p$  (energy used in photosynthesis). The regression slopes averaged  $0.89 \pm 0.08$ , implying a fairly good closure of the energy balance.

We used values of daily ET flux, called observed-ET for 2003, 2005, 2007, 2009, 2011, and 2013 from the US-Ne2 (41.165° N, 96.470° W, 362 m; <http://ameriflux.lbl.gov/sites/siteinfo/US-Ne2>) irrigated maize-soybean rotation field and from the US-Ne3 (41.180° N, 96.440° W, 363 m; <http://ameriflux.lbl.gov/sites/siteinfo/US-Ne3>) rainfed maize-soybean rotation field.

Conservation tillage practices were used, so plant residues were not ploughed into the soil, and

the soil surface was generally partially covered with prior soybean crop residue. Both sites are part of the Ameriflux (<https://ameriflux.lbl.gov/sites>) U.S. surface gas flux observation system, and the two sites are within 1.6 km of each other. The cultivars were Pn33B51, Pn33G66, Pn33H26, Pn33T57, DK\_61-72, and DK\_62-98 used in 2003, 2005, 2007, 2009, 2011, and 2013, respectively. The irrigated crops were planted on 14 May, 2 May, 1 May, 21 April, 17 May, and 30 May, and the rainfed crops on 13 May, 26 April, 2 May, 22 April, 2 May, and 13 May in 2003, 2005, 2007, 2009, 2011, and 2013, respectively. Destructive measurements of green leaf area index (LAI) and biomass were made approximately bi-monthly during the growing season.

#### *2.1.2 USDA, Agricultural Research Service, Conservation and Production Research Laboratory, Bushland, Texas, USA*

Maize was grown in 2013 and 2016 at the USDA-ARS Conservation and Production Research Laboratory (<https://www.ars.usda.gov/plains-area/bushland-tx/cprl/>), Bushland, Texas (35.18° N, 102.10° W, 1170 m above MSL) on a gently sloping (<0.3%) Pullman soil (fine, mixed, superactive, thermic Torrtic Paleustoll). Additional details and data are provided by Evett et al. (2019, 2020, 2022). Four 4.4 ha fields, approximately square in shape and adjacent to each other, each contained a large (3 m × 3 m in surface area, 2.3 m deep) precision weighing lysimeter in the center. The lysimeters contained undisturbed cores of the Pullman soil obtained on site, and they had an accuracy of 0.04 mm water depth equivalent or better (Evett et al., 2012; Marek et al., 1988). The fields and their associated lysimeters were designated NE, SE, NW, and SW according to the inter-cardinal directions. The NE and SE lysimeters and fields were irrigated by subsurface drip irrigation (SDI), and the NW and SW lysimeters and fields were irrigated by mid-elevation sprinkler application (MESA) using a ten-span linear-move system described by

Evett et al. (2019). Adaptation of SDI for the NE and SE weighing lysimeters was described by Evett et al. (2018a). A 109-day drought-tolerant variety (Pioneer 1151AM AquaMax,  $\leq 80\%$  Bt) was planted on 16-17 May 2013 under MESA irrigation, on 22-23 May 2013 in the SDI fields and on 10-11 May 2016 in all fields. These are typical dates for maize planting in the region. Crops were managed and fertilized for high grain yield, as detailed by Evett et al. (2019). In each field, destructive subsampling for leaf area index and biomass occurred in replicate plots periodically during the season, and plant height and row width were measured at the same times. Maize harvests were on 15 October 2013 and on 13 and 17 October 2016.

Soil water content was sensed at center depths of 0.10 to 2.30 m in 0.20 m increments in each of eight access tubes in the field around each lysimeter and in two access tubes in each lysimeter (to 1.90 m depth) on a weekly basis, unless prevented by wet field conditions, using a field-calibrated neutron probe and depth-control stand (Evett et al., 2008). Once the crop was established, irrigations were scheduled weekly to replenish the soil water in the top 1.5 m of the profile to field capacity (i.e., replenishing 100% of crop ET), except for one MESA field where irrigations were 75% of full crop ET after crop establishment. As explained by Evett et al. (2019), the MESA 75% deficit irrigation treatment was established to complete a previous longer-term deficit irrigation study. In some cases, two or even three irrigations were required in a week to replenish the water used by the crop. Irrigations by sprinkler and by SDI typically did not occur on the same day. Neutron probe readings were delayed until the soil surface was dry enough to walk on. The soil profile in early 2013 was quite dry, and SDI preplant irrigation and SDI irrigation immediately after planting were required to plant and germinate the crop. This resulted in a full soil profile in the SDI fields by the time neutron probe sensing began, while

crop germination with MESA irrigation was accomplished with less frequent irrigations that did not penetrate to the 1.5 m depth. Irrigations in the 100% SDI and MESA fields maintained the soil water depletion to less than the management-allowed depletion level throughout the season. In 2016, the soil profile was much wetter following a wet winter, and no preplant irrigation and less irrigation immediately after planting were needed. Again, irrigations in the 100% SDI and MESA fields kept soil water depletion to less than the management-allowed depletion level.

Evapotranspiration (ET) was determined on 5 min, 15 min, and daily bases using data analyses and quality control procedures described by Marek et al. (2014) and Evett et al. (2019). Fifteen-minute-average weather data were output from the research weather station of the USDA-ARS Soil and Water Management Research Unit at Bushland, Texas located immediately east of the lysimeter fields. The weather station instrumentation and data quality assurance and control procedures were applied as described by Evett et al. (2018b).

## *2.2 Modeling methodology*

*2.2.1 Model list.* The simulations were conducted by 20 modeling groups from around the world with 41 models completing the inter-comparison (Table 1). Details about each model are presented in supplementary Table S1. However, as can be seen from the names (Tables 1, S1), in some cases there were several “flavors” of different simulation methods tested within the same model family that were chosen by the user at run time. The biggest example is that of the DSSAT family (Hoogenboom et al., 2019a,b; Jones et al., 2003) of the Cropping System Model (CSM) within which both the CSM-CERES-Maize and CSM-IXIM-Maize (hereafter simply called CERES and IXIM) modules were run. Both calculate a value called potential evapotranspiration, ET<sub>p</sub>, which was done using four methods: (1) FAO-56 (Allen et al., 1998),

(2) Priestley-Taylor (1972), (3) the ASCE Standardized Reference Evapotranspiration Equation (Allen et al., 2005) for 12-cm grass (short crop), and (4) the ASCE Equation for 50-cm alfalfa (tall crop; *Medicago sativa* L.) with FAO-56 dual crop coefficients for maize (Table S1). Within these eight combinations, two E methods for calculating soil water evaporation were tested: “Ritchie” (Ritchie, 1972) and “Suleiman” (Suleiman and Ritchie, 2003, 2004). In addition, within the CERES-FAO-56 and CERES-Priestley-Taylor combinations, E was also computed using Hydrus (Šimůnek et al., 1998, 2008; Shelia et al., 2018), in which soil water moves based on potential gradients. Thus, there were a total of 18 (2 models x 4 ETp methods x 2 soil E methods + 2 Hydrus) DSSAT flavors. Within the DSSAT flavors, model calibrations though Phase 4 were aimed at the best statistics [lowest RMSE, and highest D-statistic (Willmont, 1982)] for growth, grain yield, ET, and soil water variables, averaged over four ET options (two ET by two E methods) in order to minimize bias. The ASCE and Hydrus ET options were not included in this process because the methods were not part of the DSSAT V4.7 release, so they were at a slight disadvantage because they were not independently calibrated. Nevertheless, the resulting cultivar coefficients were consistently used among all the DSSAT simulations.

In addition, Expert-N had GECROS and SPASS flavors, STICS had KETP and ETP\_SW flavors, and MAZSIM had daily and hourly flavors.



Table 1. List of models and their acronyms. (For details about the evapotranspiration aspects of each, see Supplementary Table S1: List of Models Plus Their Simulation Characteristics and Comparisons of Soil Moisture Simulations)

| Acronym | Model Name   | Reference               |
|---------|--|-------------------------|
| AHC     | Agro-Hydrological & chemical & Crop sys. simulator | Williams et al., 1989   |
| AMSW    | APSIM-SOILWAT                                      | Keating et al., 2003    |
| AQCP    | AquaCrop   | Allen et al., 1998      |
| AQY     | Aqyield  | Constantin et al., 2015 |
| ARMO    | ARMOSA   | Perego et al., 2013     |
| BIOM    | Biome-BGCMuSo 6.0.2                                | Hidy et al., 2016       |
| CS      | CropSyst4  | Stöckle et al., 2003    |
| DACT    | DayCent-CABBI                                      | Moore et al., 2020      |
| DCAR    | DSSAT CSM-CERES-Maize ASCE-Alfalfa Ritchie         | DeJonge & Thorp, 2017   |
| DCAS    | DSSAT CSM-CERES-Maize ASCE-Alfalfa Suleiman        | DeJonge & Thorp, 2017   |
| DCFH    | DSSAT CSM-CERES-Maize FAO-56 Hydrus                | Shelia et al., 2018     |
| DCFR    | DSSAT CSM-CERES Maize FAO-56 Ritchie               | Sau et al., 2004        |
| DCFS    | DSSAT CSM-CERES-Maize FAO-56 Suleiman              | Sau et al., 2004        |
| DCGR    | DSSAT CSM-CERES-Maize ASCE-Grass Ritchie           | DeJonge & Thorp, 2017   |
| DCGS    | DSSAT CSM-CERES-Maize ASCE-Grass Suleiman          | DeJonge & Thorp, 2017   |
| DCPH    | DSSAT CSM-CERES-Maize Priestley-Taylor Hydrus      | Shelia et al., 2018     |
| DCPR    | DSSAT CSM-CERES-Maize Priestley-Taylor Ritchie     | Sau et al., 2004        |
| DCPS    | DSSAT CSM-CERES-Maize Priestley-Taylor Suleiman    | Sau et al., 2004        |
| DIAR    | DSSAT CSM-IXIM-Maize ASCE-Alfalfa Ritchie          | DeJonge & Thorp, 2017   |
| DIAS    | DSSAT CSM-IXIM-Maize ASCE-Alfalfa Suleiman         | DeJonge & Thorp, 2017   |
| DIFR    | DSSAT CSM-IXIM-Maize FAO-56 Ritchie                | Sau et al., 2004        |
| DIFS    | DSSAT CSM-IXIM-Maize FAO-56 Suleiman               | Sau et al., 2004        |
| DIGR    | DSSAT CSM-IXIM-Maize ASCE-Grass Ritchie            | DeJonge & Thorp, 2017   |

| Acronym | Model Name                                     | Reference                |
|---------|--|--------------------------|
| DIGS    | DSSAT CSM-IXIM-Maize ASCE-Grass Suleiman       | DeJonge & Thorp, 2017    |
| DIPR    | DSSAT CSM-IXIM-Maize Priestley-Taylor Ritchie  | Sau et al., 2004         |
| DIPS    | DSSAT CSM-IXIM-Maize Priestley-Taylor Suleiman | Sau et al., 2004         |
| ECOS    | ecosys   | Grant & Flanagan, 2007   |
| JUL     | JULES  | Best et al., 2011        |
| L5SH    | L5-SLIM-H                                      | Wolf, 2012               |
| MZD     | MAIZSIM Daily                                  | Yang et al., 2009        |
| MZH     | MAIZSIM Hourly                                 | Yang et al., 2009        |
| SLUS    | SALUS  | Basso & Ritchie, 2015    |
| SLFT    | SIMPLACE LINTUL5 FAO56 SLIM3 CanopyT           | Wolf, 2012               |
| SMET    | SIMETAW#                                       | Mancosu et al 2016       |
| SSMi    | SSM-iCROP                                      | Soltani & Sinclair, 2012 |
| STCK    | STICS_KETP                                     | Brisson et al., 2003     |
| STSW    | STICS_ETP_SW                                   | Brisson et al., 2003     |
| SWB     | SWB  | Annandale et al., 2000   |
| TMOD    | Test Model                                     |                          |
| XNGM    | Expert-N - GECROS                              | Priesack et al., 2006    |
| XNSM    | Expert-N - SPASS                               | Priesack et al., 2006    |

2.2.2 *Simulation protocol.* The study was conducted in four phases:

1. “Blind phase.” The modelers were sent key input data about soils, weather, and management (planting dates, irrigations, fertilizer applications, etc.) information. They also received anthesis and maturity dates, but no other information about plant growth, grain yield, or water use.
2. “Potential or non-stressed growth phase”. The modelers were sent time-series leaf area index (LAI) and biomass observations, as well as final grain yields for all the non-water-stress treatments (only irrigated for Mead; only 100% irrigation for Bushland)
3. “Non-stress ET phase”. The modelers were sent all ET, soil water, and soil temperature for the non-water-stress treatments (only irrigated for Mead; only 100% irrigation for Bushland)
4. “All phase”. In this final phase, the modelers were provided with all LAI, biomass, grain yield, ET, soil moisture, soil temperature etc. data for all treatment-years.

The modelers were told to start their simulations on day-of-year 91, so there would be time for equilibration of soil moisture and soil temperature. They were also provided “initial” soil water content profiles, but the number of days before planting at which soil moisture was determined varied widely from season to season.

### 2.2.3 *Methods for evaluating model performance*

Correlation coefficients ( $r$ ), D statistics (Willmott, 1982), root mean squared errors between observed and simulated values (RMSE), normalized root mean squared errors (nRMSE), average differences, as well as mean squared deviations (MSD), standard bias (SB), non-unity of slopes

(NU), and lack of correlations (LC) following Gauch et al. (2003), are all presented as Supplementary Statistical Data for Phase 4. Also included are slopes and intercepts of regressions of observed on simulated data, along with corresponding graphs for each model and analyzed parameter.

Herein, we chose to present the nRMSE results calculated using:

$$\text{nRMSE} = \{[n^{-1} \sum (P_i - O_i)^2]^{0.5}\} \bar{O}^{-1}$$

where  $n$  = number of observations,  $P_i$  and  $O_i$  are the simulated and observed  $i$ th value pair, and  $\bar{O}$  is the observed mean. Normalizing with  $\bar{O}$  enables a comparison of the variability of parameters with widely different units and scales, such as ET rate and biomass accumulation, although admittedly, nRMSE fails for  $\bar{O} = \text{zero}$  or small values close to zero.

#### 2.2.4 *k*-means clustering

A *k*-means clustering algorithm was used to group models with similar nRMSE statistics and identify the top-performing models in a non-arbitrary way. Analyses focused on nRMSE for four pairs of model output variables, including simulated ET (ETs) versus grain yield and biomass from -10 to +20 days after planting (DAP) (soil E dominant) and from 41 to 100 DAP (canopy T dominant). Initial tests varied the number of clusters ( $n$ ) from 1 to 19. The final analysis was conducted with  $n=4$  clusters based on reducing the sum of squared distance from the cluster center to less than 20% of that for  $n=1$  cluster. Using  $n=4$  clusters also resulted visually appealing cluster plots with the set of top-performing models clearly identified within groups having low nRMSE for both variables of each pair. The *k*-means analysis was conducted using the “scikit-learn” package for Python (Pedregosa et al., 2011).

### 3 Simulation results and discussion

#### 3.1 Daily results for irrigated and rainfed Mead in 2003 (the driest year) and Bushland 100% and 75% sprinkler irrigations in 2013 (the year with highest observed ET rates)

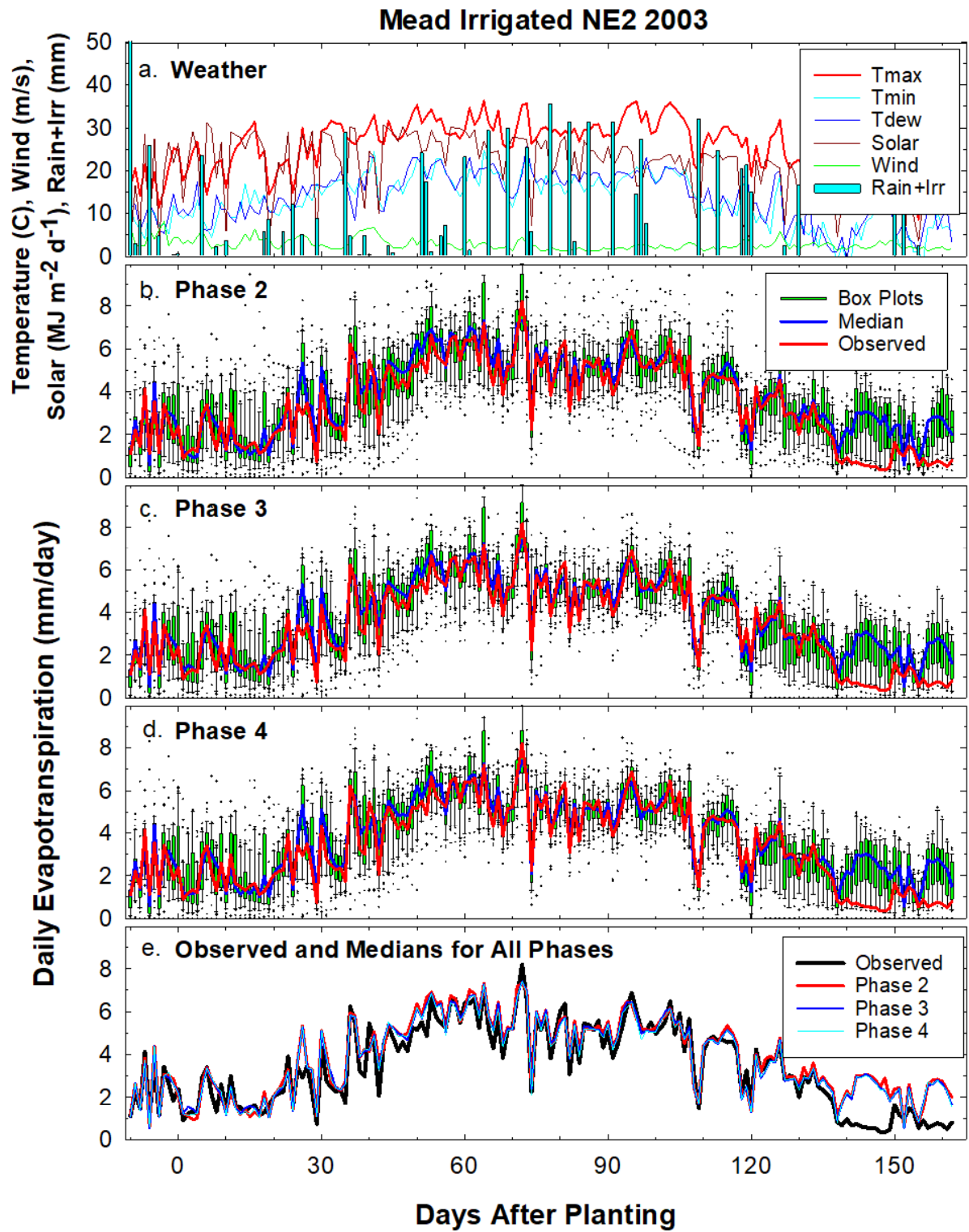
These four cases were selected from among the twenty treatment-years available for more detailed (daily) examination because they represent the two sites and the two cases at each site with the likely greatest water stress difference between treatments, i.e., irrigated versus rainfed in the driest year at Mead and 100% versus 75% MESA irrigation in the year with the highest daily ET rates in Bushland.

##### 3.1.1 Daily simulated evapotranspiration (ETs)

3.1.1.1 *Irrigated Mead in 2003.* As found previously (Kimball et al., 2019), there was a wide range in ETs among the models (Fig. 1). However, the median of all the models tended to be close to the observed values most days. Admittedly, for this intercomparison, as well as for all the others that follow in the rest of this paper, the median is biased toward DSSAT because of the large number of “flavors.” For this case, the observed values fell within the short (1-3 mm/d) green boxes much of the time, which indicates many of the models produced respectable simulations. There was only a slight ( $< 1$  mm/d) improvement in model performance going from Phase 1 to Phase 4. It appears that the greatest variability and uncertainty among the models occurred from about 10 days before planting to 10 DAP (soil E dominated) and from about 130 to 160 DAP (after the crop matured). A likely cause of the latter issue is that many models retained a fair amount of green LAI at and after simulated maturity; thus, model equations for ET that depend strongly on LAI did not result in sufficient termination of ET. Successive model adjustments or calibrations going from Phase 1 to Phase 4 as more information was provided only slightly improved this. Model code improvement is needed to decrease green LAI due to

senescence, eventually shutting down T at crop maturity. Code improvement likely is also needed to improve the simulation of bare soil ET.

3.1.1.2 *Rainfed Mead in 2003*. For rainfed conditions at Mead, the models showed large variability (uncertainty) in daily ETs from about -10 to +10 DAP (soil E dominated; Fig. 2) similar to the irrigated field (Fig. 1). The greatest deviations (or errors) occurred from about 70 to 95 DAP when there was little rainfall (Fig. 2a). The observed ET continued at close to 4 mm/d, whereas the models simulated much lower rates. Like the irrigated field (Fig. 1), after DAP 120 as the crop matured, the measured ET decreased rapidly, whereas the models continued to simulate much higher ET. The ET variability during the -10 to +10 DAP period was related to highly different methods for simulating E, some of which proved to be less accurate. The issues during the maturation period after 120 DAP are related to the insufficient termination of T after maturity. More importantly, the period from about 70 to 95 DAP and beyond corresponds to the period of water limitation, when most models (and the median) simulated lower than observed ET. We suspect this is caused by inadequate soil water dynamics in the models, such as insufficient rooting depth, inadequate water up-flux or the presence of a perched water table, as well as excessive simulated ET during the early growth phase that depleted the simulated soil water too much, thus reducing ET later.



441

442

Figure 1. (a.) Weather variables (maximum and minimum air temperature, dew point, solar radiation, wind speed, rainfall) observed at irrigated field NE2 at Mead in 2003 versus days after planting (DAP). (b.) Box plots of daily simulated evapotranspiration (ETs) where the lower and upper limits of the box indicate the 25<sup>th</sup> and 75<sup>th</sup> percentile of ET values simulated by 41 maize growth models, respectively, the lower and upper whiskers indicate the 10<sup>th</sup> and 90<sup>th</sup> percentiles, and the points are outliers. Observed values and the median values from the 41 models are also shown. The simulated outputs start with Phase 2, for which the modellers were given leaf area index, growth, and grain yield data for all 100% irrigated treatment-years. Phase 1 simulations, a “blind” test whereby the modellers were only given weather, phenology, management, and soils information, are missing from this graph because a plant population mistake was made for Mead irrigated fields. (c.) Same as (b.) except for Phase 3 whereby the modellers were given the observed ET, soil water content, soil temperature for all 100% irrigated treatment-years. (d.) Same as (c.) except for Phase 4 whereby the modellers were given all data, including ET, growth, and grain yield, for all 20 treatment-years, including rainfed and 75% irrigations. (e.) Observed daily ET values as well as the median ETs values for Phases 2, 3, and 4



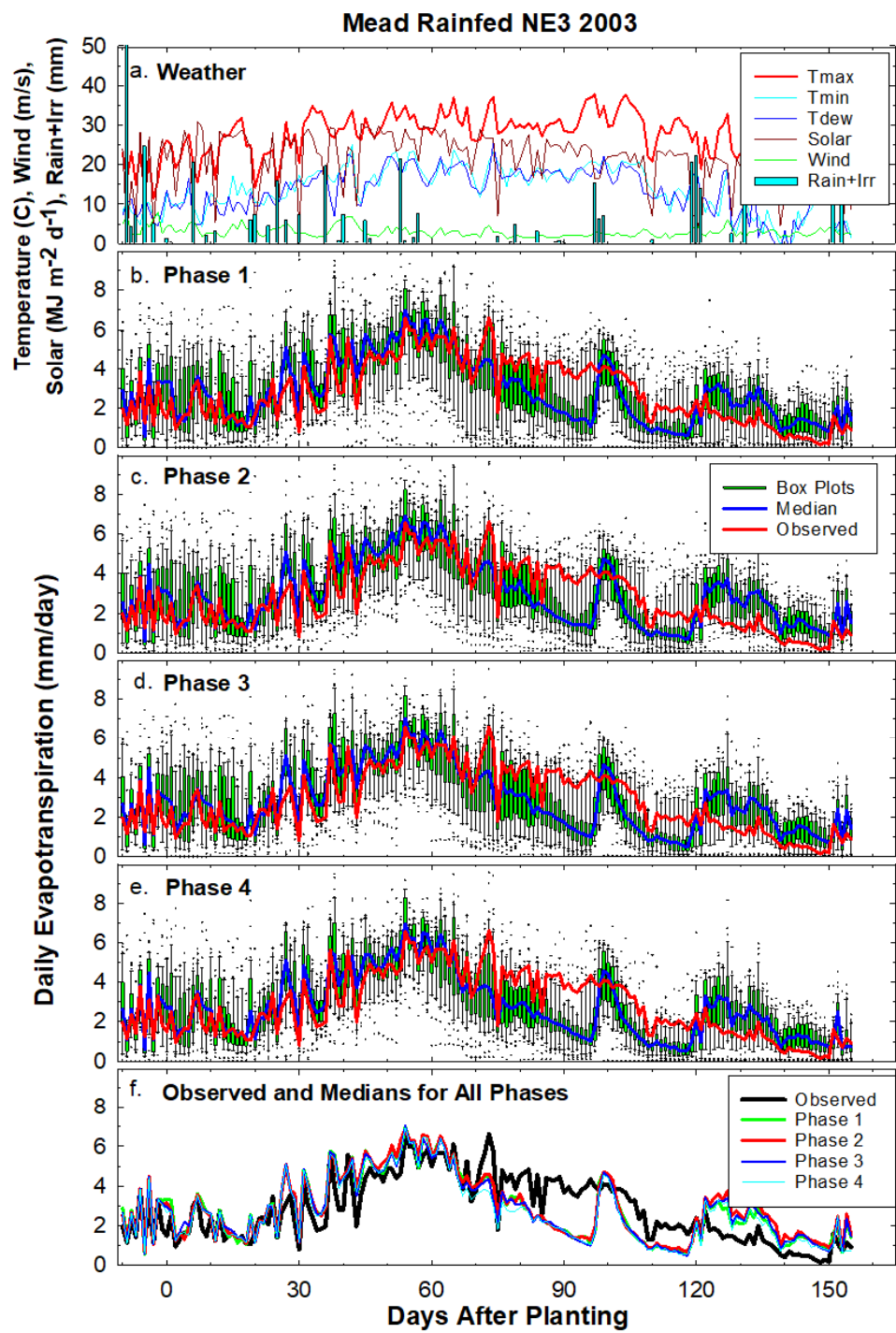


Figure 2. Similar to Figure 1 except for rainfed Mead field NE3 in 2003, and data for Phase 1 are also included.

3.1.1.3 *100% and 75% irrigated Bushland in 2013*. For the Bushland location, most of the models (and the median) under-estimated ET during the 45 to 80 DAP period when windspeeds were high ( $> 5$  m/s) and dew points were low (Figs. 3, 4). Model calibration (Phases 1 to 4) only partially improved this situation. This is possibly related to the fact that many of the models do not adequately account for varying wind speed and humidity, as can be deduced from the fact that the models estimated ET fairly well during periods of smaller ET but under-estimated ET greatly during periods of larger ET, when wind speeds were high and relative humidity was low. The fact that solar irradiance was also smaller during some of the periods of smaller ET (due to storm fronts) indicates that the radiation and energy balance algorithms may also need improvement. As before with Mead (Figs. 1, 2), the models failed to reduce T sufficiently after crop maturation (Figs. 3, 4; 105 to 145 DAP). Surprisingly, the models tended to simulate the 75% irrigation treatment (Fig. 4) better than they did the 100% treatment (Fig. 3). Again, we speculate that this is because many of the models had not been calibrated previously to account for the very high winds and low humidity in Bushland, so their ETs simulations were lower than the high observed ET rates for the 100% irrigations treatment (Fig. 3), whereas under the 75% treatment (Fig. 4), drought stress reduced observed ET rates into the ranges for which the models had been calibrated. The fact that observed ET for the 75% MESA irrigations treatment was similar to that for the 100% SDI treatment (Evet et al., 2019) indicates that E may play an important role in the discrepancies between simulated and observed ET for the 100% MESA treatment. The major difference between SDI and MESA irrigation in the Bushland experiments was the larger evaporative losses from the soil surface in MESA irrigated fields (Evet et al., 2019).

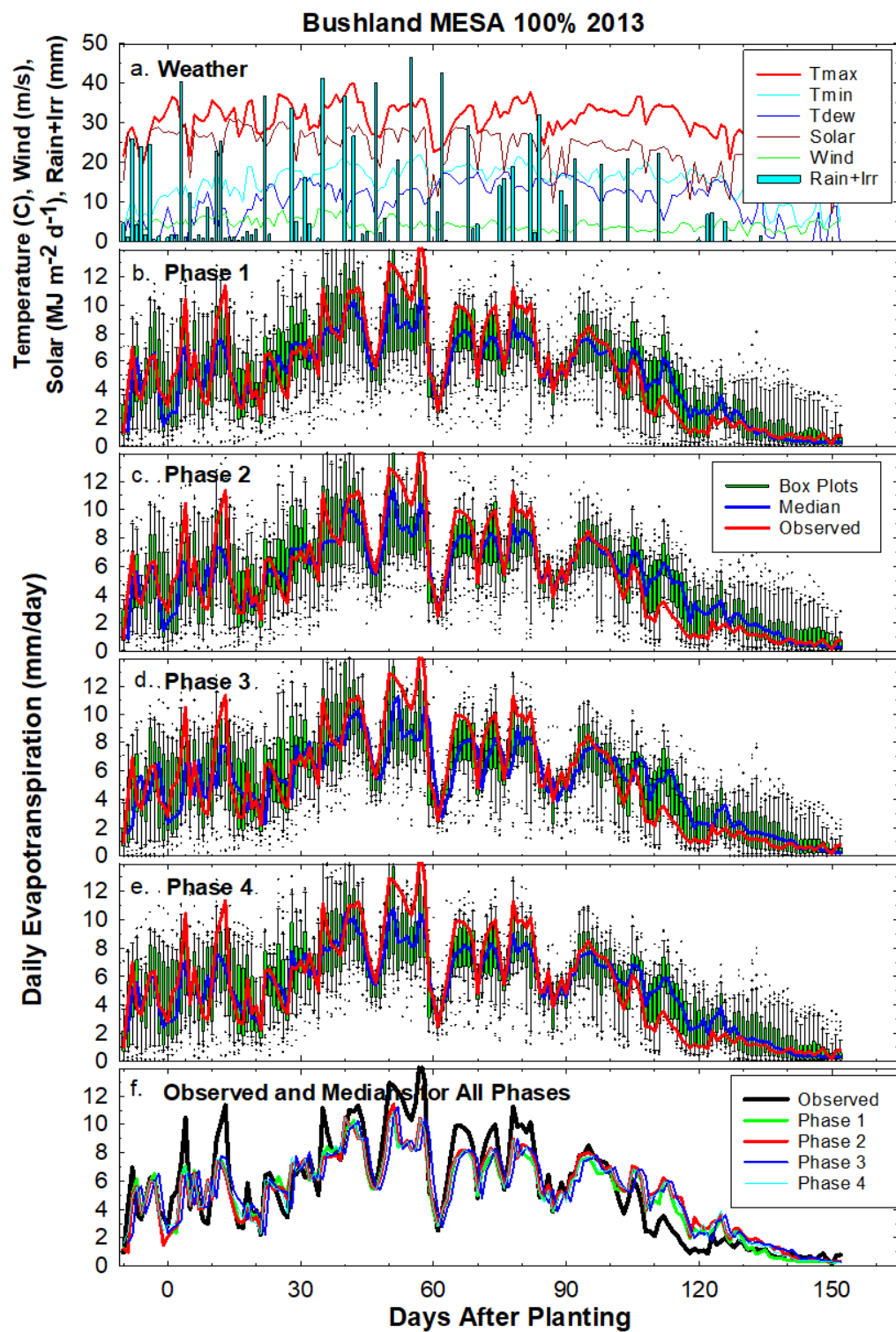


Figure 3. Similar to Fig. 1 except for 100% MESA (mid-elevation sprinkler application) irrigation at Bushland in 2013.

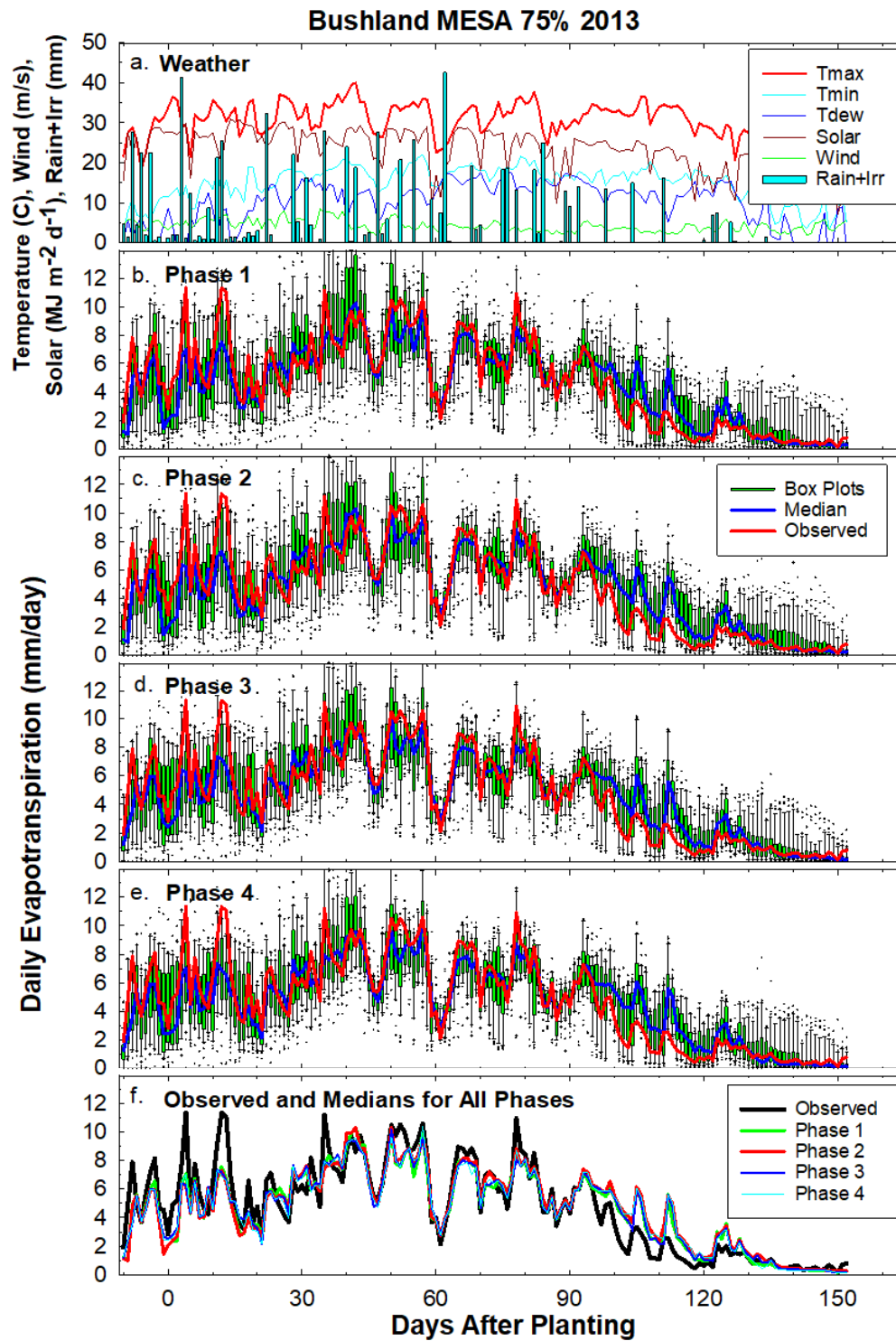


Figure 4. Similar to Fig. 1 except for 75% irrigation at Bushland in 2013, and data for Phase 1 are also included.

### 3.1.2 Ranking of models with respect to their nRMSE for simulating daily ETs

#### 3.1.2.1 Irrigated Mead in 2003

The median of all the models had the lowest nRMSE for ETs for Phases 2, 3, and 4 for both early season (-10 to +20 DAP; soil E dominant) and mid-season (41 to 100 DAP; canopy T dominate) (Fig. 5). For early season STCK was the best model followed by several DSSAT “flavors,” and at mid-season several DSSAT flavors again did well, especially for Phase 2. STCK uses Penman (1948) to calculate atmospheric demand and the 2-phase model of Brisson and Perrier (1991) and Brisson et al. (1998, 2003) to calculate soil water evaporation,  $E_a$  (Table S1). Note that all the DSSAT flavors listed for -10 to +20 DAP end in “R”, which indicates that the soil E method of Ritchie (1972) was better than the more recent method of Suleiman and Ritchie (2003, 2004). However, for Phase 2 during the 41 to 100 DAP period DIFS and DCFS did well, but during this period canopy T was dominant, so soil E was relatively unimportant then.

The effects of changes made by the modelers going from phase to phase can also be seen in Fig. 5. For example, BIOM was ranked 19<sup>th</sup> for Phase 2, -10 to +20 DAP but improved to 5<sup>th</sup> and 6<sup>th</sup> for Phase 3 and Phase 4, respectively. Like the well-performing DSSAT flavors, BIOM

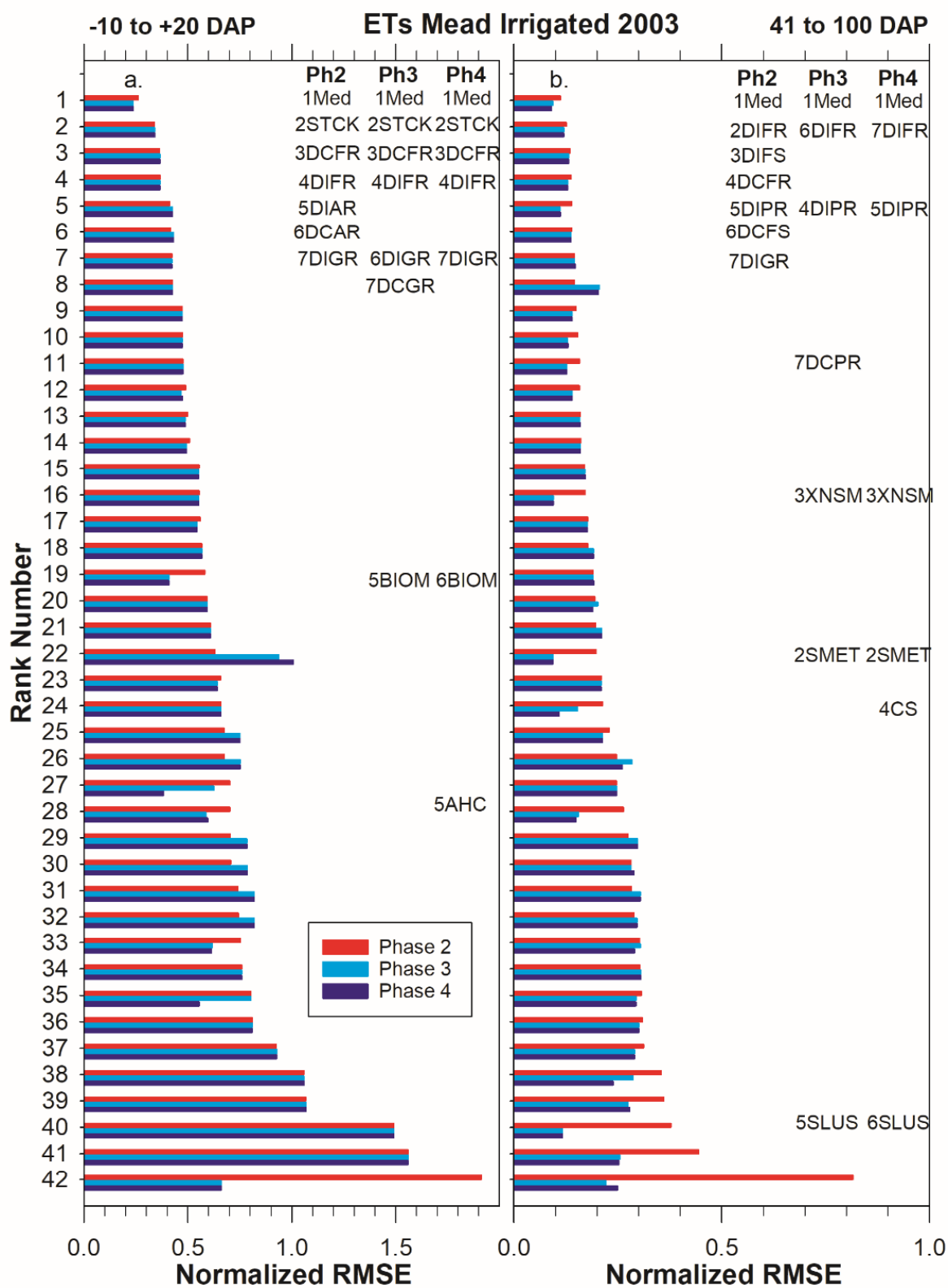


Figure 5. (a) Normalized root mean squared error (nRMSE) between observed and simulated daily ET values from -10 to +20 days after planting (DAP)(mostly soil E) for the irrigated field NE2 at Mead in 2003 for all the models. Phases 2, 3, and 4 are identified by red, cyan, and blue bars with Phase 2 at the top and Phase 4 at the bottom of each group. Phase 1 data are missing from this graph because a plant population mistake was made for Mead irrigated fields. The models have been sorted in ascending order of nRMSE for Phase 2 from top to bottom of the graph with the rank numbers on the left axis indicating their ranking for Phase 2. The Median (Med) and the six best models (lowest nRMSE) for Phase 2 are listed under “Ph2”. Somewhat similarly, the Median and six best models for Phases 3 and 4 are also listed under “Ph3” and “Ph4”, but because the modelers made different adjustments going from phase to phase, their rank order changed, so the names along with their nRMSE rank are in different positions down the graph. (b) Same as for (a) except the data are for 41 to 100 DAP (mostly crop canopy T) with the ranking done on the 41 to 100 DAP Phase 2 data

also uses Ritchie (1972) to simulate soil E. AHC rose from 28<sup>th</sup> to 5<sup>th</sup> from Phase 2 to Phase 4 for the -10 to +20 period. AHC uses the two-stage FAO-56 method to simulate E for mostly bare soil (Table S1). A huge improvement was made by SLUS going from 40<sup>th</sup> for Phase 2 to 5<sup>th</sup> for Phase 3 for the 41 to 100 DAP period. SLUS calculates atmospheric demand from Priestly and Taylor (1972) and then uses an empirical equation to simulate potential ET<sub>p</sub> (Table S1), which would be mostly T for the irrigated full canopy. XNSM, SMET, and CS all markedly improved from Phase 2 to Phase 4 to be among the best for the full canopy (Fig. 5b). All three use FAO-56 (Allen et al., 1998) with some modifications (Table S1).

#### 3.1.2.2 *Rainfed Mead in 2003*

The STCK model was best for simulating ETs for the -10 to +20 DAP period in the rainfed field at Mead in 2003 for Phases 1 and 2, while the median was 2<sup>nd</sup>, and then they traded rankings for Phases 3 and 4 (Fig. 6a). ECOS, JUL, DCFR, DIFR, and STSW also did very well. ECOS is a full energy balance model while JUL uses the Penman-Monteith approach (Monteith, 1965) with a 10-layer canopy (Table S1). BIOM rose from 31<sup>st</sup> for Phase 1 to 3<sup>rd</sup> for Phases 3 and 4. JUL and XNGM were best for the 41 to 100 DAP period (Fig. 6b). MZD was 3<sup>rd</sup> for Phase 1, but did much worse in the other phases. DIFR, DCFR, and DIPR did well. ECOS rose from 13<sup>th</sup> for Phase 1 to 2<sup>nd</sup> for Phases 3 and 4. All of these listed models were better than the median for this case.

#### 3.1.2.3 *100% MESA irrigation at Bushland in 2013*

The median of all the models ranked 1<sup>st</sup> at simulating ETs from -10 to +20 DAP for all phases in Bushland with 100% MESA irrigation in 2013 (Fig. 7a). Except for Phase 2, ECOS, an energy



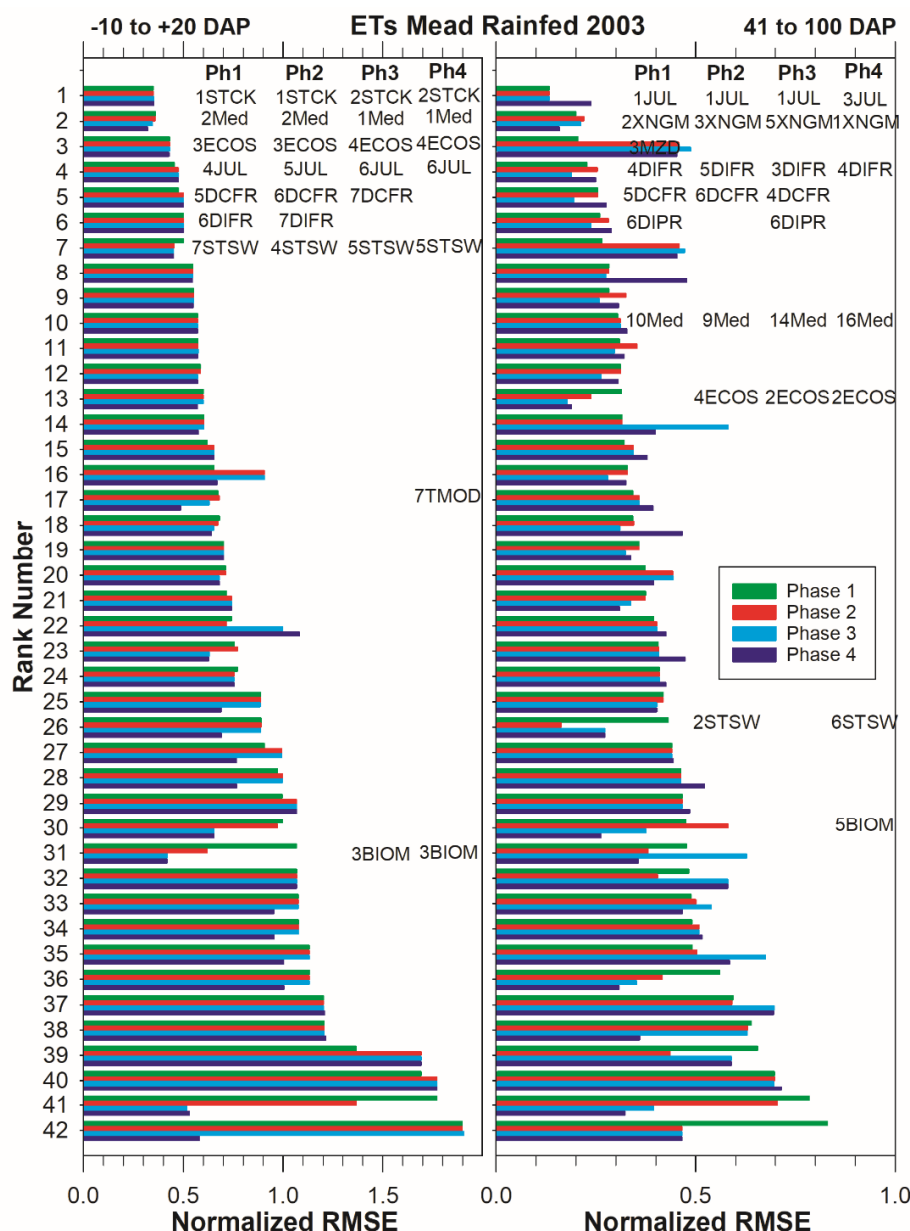
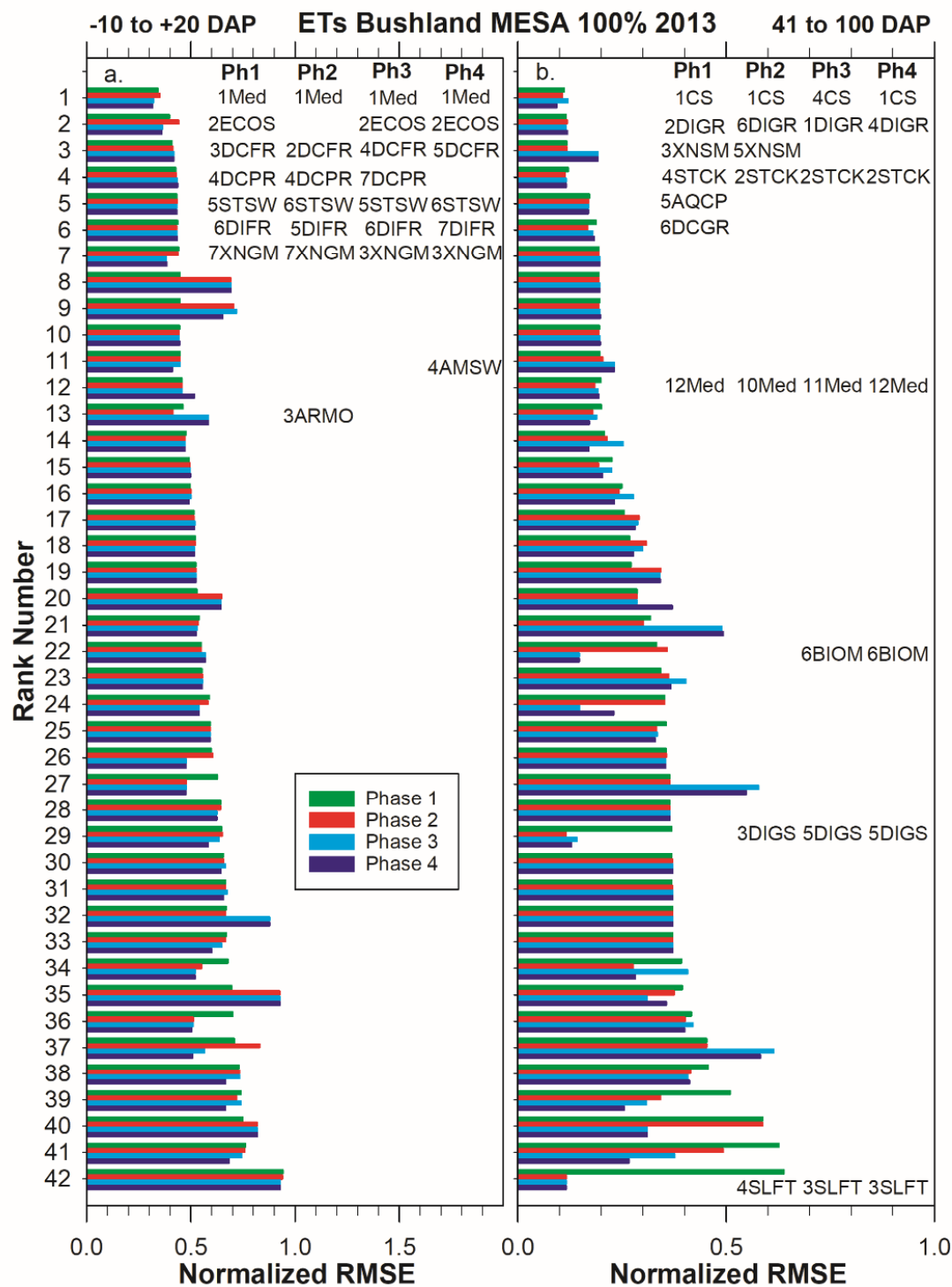


Figure 6. (a.) Normalized root mean squared error (nRMSE) between observed and simulated daily ET values from -10 to +20 days after planting (DAP)(mostly soil E) for the rainfed field NE3 at Mead in 2003 for all the models. Phases 1, 2, 3, and 4 are identified by green, red, cyan, and blue bars with Phase 1 at the top and Phase 4 at the bottom of each group. The models have been sorted in ascending order of nRMSE for Phase 1 from top to bottom of the graph with the rank numbers on the left axis indicating their ranking for Phase 1. The Median (Med) and the six best models (lowest nRMSE) for Phase 1 are listed under “Ph1”. Somewhat similarly, the Median and six best models for Phases 2, 3 and 4 are also listed under “Ph2”, “Ph3”, and “Ph4”, but because the modelers made different adjustments going from phase to phase, their rank order changed, so the names along with their nRMSE rank are in different positions down the graph. (b.) Same as for (a.) except the data are for 41 to 100 DAP (mostly crop canopy T).



562

563 Figure 7. Like Fig. 6 except for 100% MESA (mid-elevation sprinkler application) irrigation to  
564 restore soil water to field capacity at Bushland.

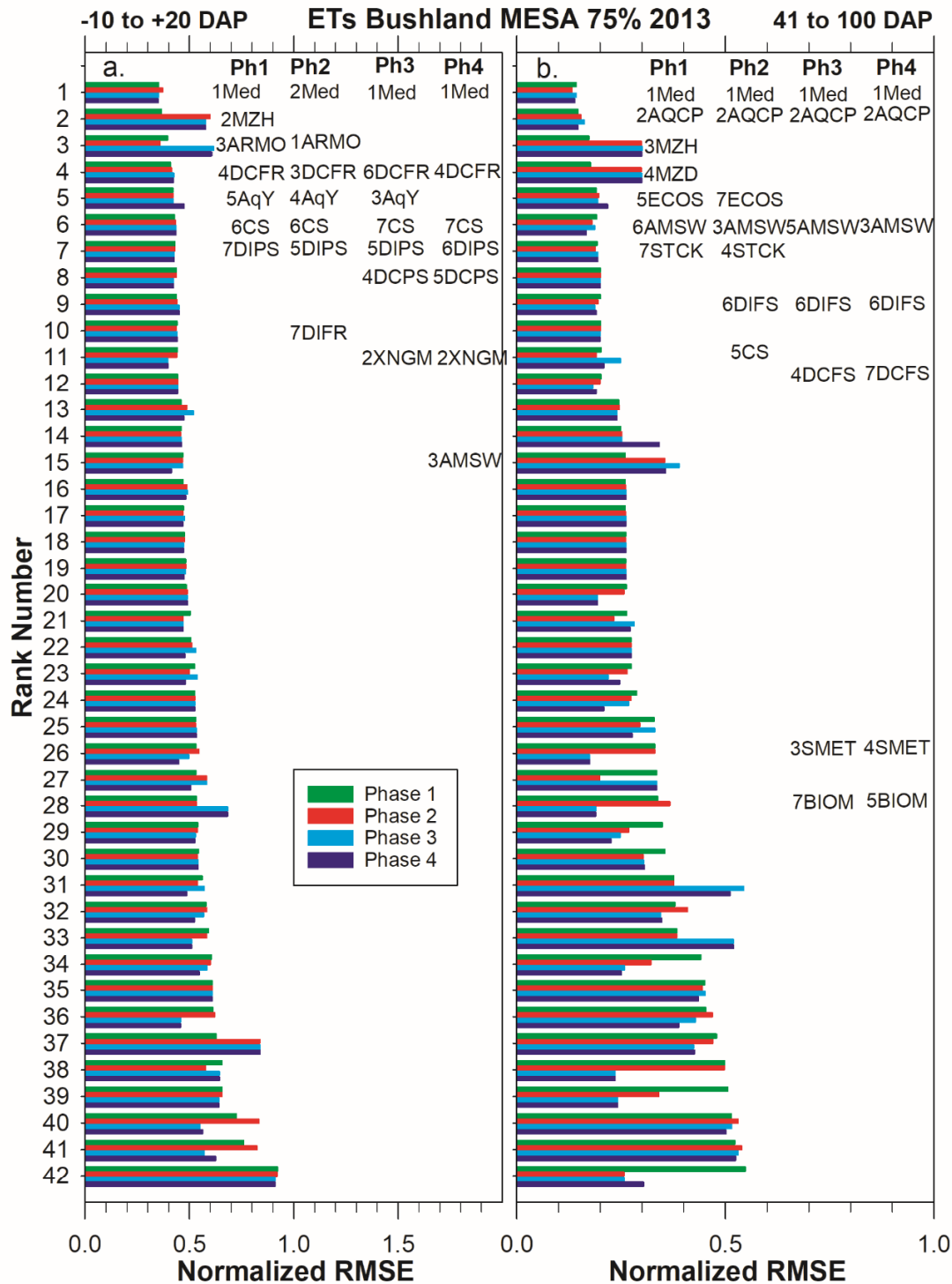


Figure 8. Like Fig. 6 except for the MESA (mid-elevation sprinkler application) 75% irrigation at Bushland.

balance model was best. DCFR, DCPR, STSW, DIFR, and XNGM all did well. At mid-season (41 to 100 DAP, Fig. 7b), CS, DIGR, and STCK did well for all phases. BIOM and DIGS improved greatly for phases 3-4. However, the median was only about 12<sup>th</sup>.

#### 3.1.2.4 75% MESA irrigation at Bushland in 2013

The median of all the models was 1<sup>st</sup> for all but one phase for both early season (-10 to +20 DAP) and mid-season (41 to 100 DAP) for the 75% irrigation treatment at Bushland in 2013 (Fig. 8). MZH was ranked 2<sup>nd</sup> for Phase 1, early season (Fig. 8a) but then did much worse for other phases. Similarly, ARMO did well for Phases 1 and 2, but then did much worse. DCFR, CS, and DIPS did well in all phases. XNGM, AMSW, and DCPS were among the best for Phase 4. AMSW uses a transpiration efficiency to compute ETs from biomass accumulation, XNGM uses a modified Penman-Monteith (Monteith (1965), and DCPS uses Priestly and Taylor (1972) to simulate potential atmospheric demand and ultimately ETs.

At mid-season, AQCP and AMSW did well for all phases (Fig. 8b). MZH and MZD did well for Phase 1, but then much worse for later phases. DIFS, DCFS, SMET, and BIOM did well for Phases 3 and 4.

#### 3.1.2.5 Intercomparison among the models for all four cases of daily ET for Phase 4

Looking at Figs. 5-8, no single model appears among the best (lowest nRMSE) six for all four cases. The median was among the best for the all four cases from -10 to +20 DAP (mostly E), but only for two cases from 41 to 100 DAP (mostly T). Focusing on the -10 to +20 periods (mostly E), DCFR was among the best for 3 cases; STCK, DIFR, BIOM, ECOS, STSW, SNGM,

and AMSW for 2 cases; and DIGR, JUL, TMOD, CS, DIPS, DCPS for 1 case. For the 41 to 100 DAP periods, the median was among the best only twice. BIOM was best for 3 cases; DIFR, CS, and SMET were best for 2 cases; and STCK DIGR, ECOS, JUL, STSW, XNGM, DIPR, XNSM, SLUS, DIGS, SLFT, AQCP, AMSW, DIFS, and DCFS were all among the best for 1 case. BIOM stands out as being the only model to be among the best twice for early season (mostly E) and thrice for midseason (mostly T).

### 3.2 *Inter-comparisons within the DSSAT family*

#### 3.2.1 *Daily ETs*

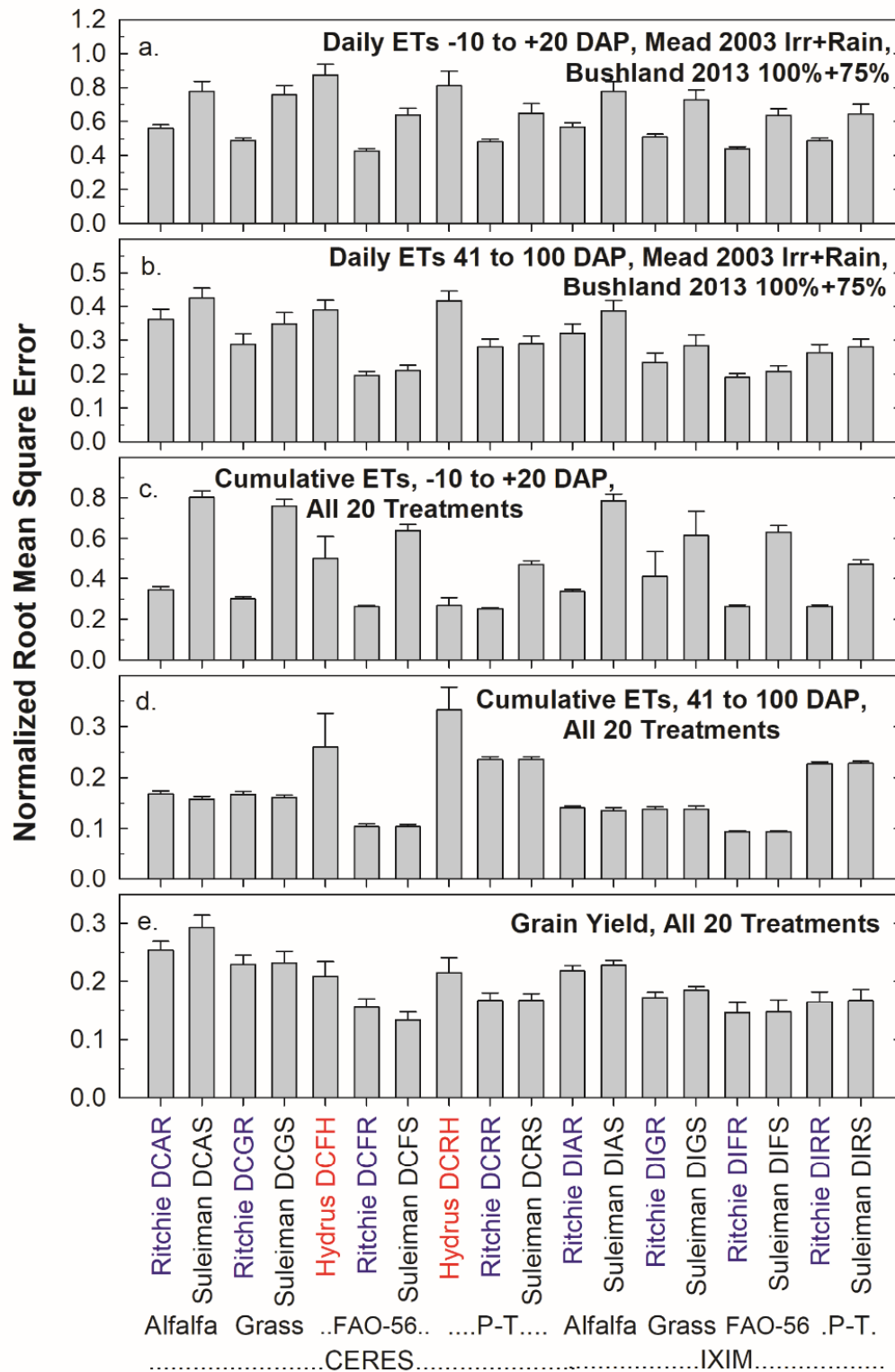
A comparison of E methods within the DSSAT models, revealed that the older Ritchie-2-stage model (Ritchie, 1972) was consistently better (lower nRMSE and lower simulated ETs) than the Sulieman and Ritchie method (2003, 2004) during the -10 to +20 DAP period, regardless of the other ET methods (Figs. 9a, 10a). The Ritchie-2-stage method was also better (slightly lower nRMSE) for ETs in the 41 to 100 DAP full canopy phase (Figs. 9b, 10b) for two reasons (less E during that phase, but mostly because lower early E allowed soil water in deeper layers to be conserved for the 41 to 100 DAP period, thus contributing more to T during the latter phase).

In spite of having a theoretically more realistic mechanism for moving soil water with potential gradients, the Hydrus method (Šimůnek et al., 1998, 2008; Shelia et al., 2018) did not perform as well as the more empirical Ritchie (1972) and Sulieman and Ritchie (2003, 2004) methods (Fig. 9a, 9b). However, Hydrus was just recently incorporated into the DSSAT shell, whereas the Ritchie (1972) and the Sulieman and Ritchie (2003, 2004) routines have been used for many years and likely have been fine-tuned to the system. Also, Hydrus is very sensitive to the values

616 of the soil physical and hydraulic properties, so if those parameter values were off, the simulated  
617 ET would also be off.

618

619 A comparison of potential ET (ET<sub>p</sub>) methods within the DSSAT models illustrated that the  
620 FAO-56 method (in present DSSAT; Allen et al., 1998) with K<sub>can</sub> of 0.62 (gives K<sub>ep</sub> = 0.50)  
621 performed better (lower nRMSE) for ETs than the other ET<sub>p</sub> methods: Priestley-Taylor (P-T;  
622 1972), alfalfa reference-[ET<sub>r</sub>, ASCE equation (Allen et al., 2005)], or grass reference-[ET<sub>o</sub>,  
623 ASCE equation (Allen et al., 2005)] during both the -10 to +20 DAP period and the 41-100 DAP  
624 period (Figs. 10a, 10b). K<sub>can</sub> is the extinction coefficient for absorption of photosynthetically-  
625 active radiation by LAI, while K<sub>ep</sub> is the extinction coefficient for absorption of total solar  
626 energy by LAI. The default K<sub>can</sub> for CERES is 0.85 (in the ecotype file). K<sub>can</sub> was reduced to  
627 0.62

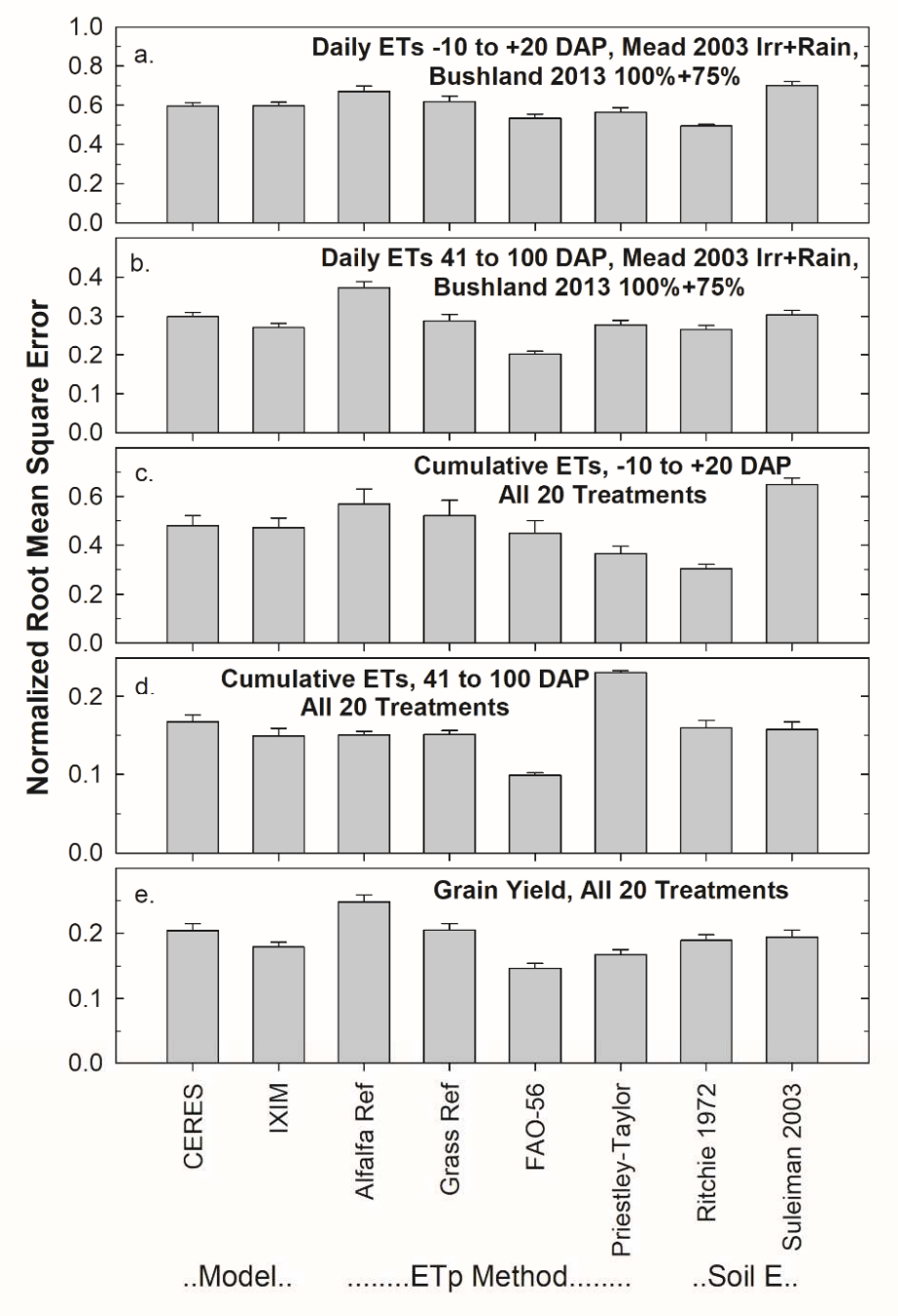


628

629

Figure 9. Normalized root mean square errors (nRMSE) of the 18 “flavors” of the DSSAT family models (a) for the -10 to +20 DAP periods (mostly soil E) of daily ETs over all phases for the irrigated and rainfed data for Mead 2003 and the 100% and 75% MESA irrigated data for Bushland 2013. Models included are DSSAT CSM-CERES and DSSAT CSM-IXIM, whose horizontal names span the corresponding left ten and right eight vertical bars, respectively. Potential ETp calculation methods are using alfalfa (tall, ET<sub>r</sub>) and grass (short, ET<sub>o</sub>) reference crop coefficients with the ASCE standardized reference equation (Allen et al., 2005), FAO-56 (Allen et al., 1998), and Priestley-Taylor (1972). These horizontal names span the corresponding bars above them. Soil evaporation calculation methods follow Ritchie (1972; labelled “Ritchie”), Suleiman and Ritchie (2003, 2004; labelled just “Suleiman”), and Hydrus (Šimůnek et al., 1998, 2008; Shelia et al., 2018; labelled “Hydrus”). (b) Like (a) except for the 41 to 100 DAP periods. (c.) The values plotted are averages (+ standard errors) of the nRMSEs for Phase 4 for all 20 treatment-years of the cumulative ETs from -10 to +20 DAP periods. (d.) Like (c.) except for the cumulative ETs from 41 to 100 DAP. (e.) nRMSEs for Phase 4 grain yields for all 20 treatments.





648  
649 Figure 10. Direct comparisons using the same data as for Fig. 9 (excluding Hydrus) between the  
650 DSSAT-CERES and DSSAT-IXIM models, among the four potential ET methods, and between  
651 the two soil water evaporation methods for the corresponding a, b, c, d, and e graphs. The  
652 horizontal “Model”, “ETp Method”, and “Soil E” labels span the corresponding bars above.  
653  
654

during phase 3, which reduces the effective energy extinction from 0.685 to 0.50 [latter value supported lysimeter studies of Villalobos and Fereres (1990), as well as the theory of foliar absorption of total solar energy (Goudriaan, 1977)]. The  $K_{ep}=0.50$  was used for P-T as well. On the other hand, the alfalfa reference-FAO-56, or grass reference-FAO-56 are dual-coefficient methods that compute their own coefficients during incomplete and full canopy phases of ET. In contrast to a previous study on cotton (*Gossypium hirsutum* L.) ET (Thorp et al., 2020), the methods based on ASCE alfalfa and grass reference ET did not perform as well as DSSAT FAO-56 and P-T; however, the calibration methodology limited their comparability in the present study. It appears that the newly reduced  $K_{ep}$  of 0.50 contributed to improved DSSAT performance, and it is an improvement over the default DSSAT value. As mentioned previously, Sau et al. (2004) reported that the FAO-56 with a  $K_{ep}=0.50$  gave the best simulations of ET, soil water extraction, and biomass accumulation with the CROPGRO-Faba bean model for a water-limited environment. FAO-56 was better than P-T, and the extinction coefficient ( $K_{ep}=0.50$ ) was better than a higher  $K_{ep}$  for either ET method. Similarly, Lopez-Cedron et al. (2008) found the CERES model gave better simulations of maize biomass, grain yield, and harvest index under water-limited environments, using FAO-56 rather than P-T, and again,  $K_{ep}$  of 0.50 was better than a higher energy extinction coefficient (default in CERES was 0.685).

There was no significant difference in nRMSE between the CERES or IXIM models for the -10 to +20 DAP period (Fig. 10a, soil E dominant), whereas for the 41 to 100 DAP period (Fig. 10b, canopy T dominated), IXIM was slightly better, likely because of its more realistic simulation of LAI progression. IXIM senesces green leaf area more rapidly (and more mechanistically) near

maturity than does CERES, which results in less T during the grain-filling phase, and which more closely matches the observed reduction in T.

Comparing methods for calculating potential evapotranspiration (ET<sub>p</sub>) on the nRMSE of ETs for the 41 to 100 days after planting (DAP) period (Fig. 10b), the FAO-56 method had significantly lower nRMSE. For the -10 to +20 DAP period (Fig. 10a), it was better than both the alfalfa (tall; *Medicago sativa* L.) and grass (short) crop coefficients with the ASCE standardized reference equation, but Priestley-Taylor (P-T) tended to be almost as good. Comparing soil E methods, Ritchie (1972) was much better than Suleiman and Ritchie (2003, 2004) for the -10 to +20 DAP period (Fig. 10a) soil E dominant), and Ritchie (1972) was slightly better even for the 41 to 100 DAP period (Fig. 10b, canopy T dominant).

### 3.3 Inter-comparisons within the STICS, Expert-N, and MAZSIM families

Comparing the nRMSE of daily ETs between the two “flavors” of each pair of the STICS, Expert-N, and MAZSIM families, there were no significant differences (Figs. 11a, 11b). STCK uses a single surface model (Penman, 1948) to compute potential ET<sub>p</sub>, whereas STSW handles separate canopy and soil surfaces (Shuttleworth and Wallace, 1985). Thus, for these four cases, STCK and STSW performed equally well at simulating soil E (Fig. 11a) and canopy T (Fig. 11b) in spite of the different methods for simulating ET<sub>p</sub>. Both XNSM and XNGM models use Penman-Monteith based approaches for simulating ET<sub>p</sub>. However, XNSM follows FAO 56 guideline based on ETo multiplied with a single crop factor to get ET<sub>p</sub> while in XNGM the required surface- and aerodynamic resistances are calculated directly from simulated LAI and simulated canopy height. In addition, XNGM follows the more detailed Farquhar model in

simulating photosynthesis and leaf T but simplifies vertical root distribution. The latter could possibly explain slightly better soil moisture simulations of XNSM compared to XNGM (data not shown). In XNSM, temperature, moisture, and nutrient availability in different soil layers are taken into account when simulating rooting depth and root length distribution. In contrast, XNGM assumes a uniform distribution of root length density within the rooted zone, with the increase in rooting depth simply simulated from the increase in root biomass, regardless of the soil conditions. Thus, considering that there are marked differences between the two models, it is surprising that they differ so little in their ability to simulate ETs. The lack of significant differences between MZD and MZH is reasonable because they are the same in their representation of plant and soil processes. Both models run on an hourly time step internally but MZD takes daily weather data as input and interpolates them into hourly time steps, while MZH takes hourly weather data directly as input.

### *3.4 Potential ET<sub>p</sub> and other sources of variability/error in daily ETs*

There was a wide variability among the models in their simulated values for daily ETs as shown in Figs. 1-4, which is similar to the previous results reported by Kimball et al. (2019). In that report, Fig. 10 shows that much of the variability can be attributed to variability among the models in their values of ET<sub>p</sub>. Therefore, for this study we requested more values of “upstream” variables that the modelers might be using to compute ET<sub>p</sub>, including reference ET based on short (12 cm) grass (ET<sub>o</sub>), reference ET based on tall (50 cm) alfalfa (ET<sub>r</sub>), soil coefficient (K<sub>s</sub>), basal crop coefficient (K<sub>cb</sub>), soil evaporation coefficient for drying soil (K<sub>e</sub>), overall crop coefficient (K<sub>c</sub>), potential soil evaporation (E<sub>p</sub>), potential transpiration (T<sub>p</sub>), ET<sub>p</sub>, and of course,

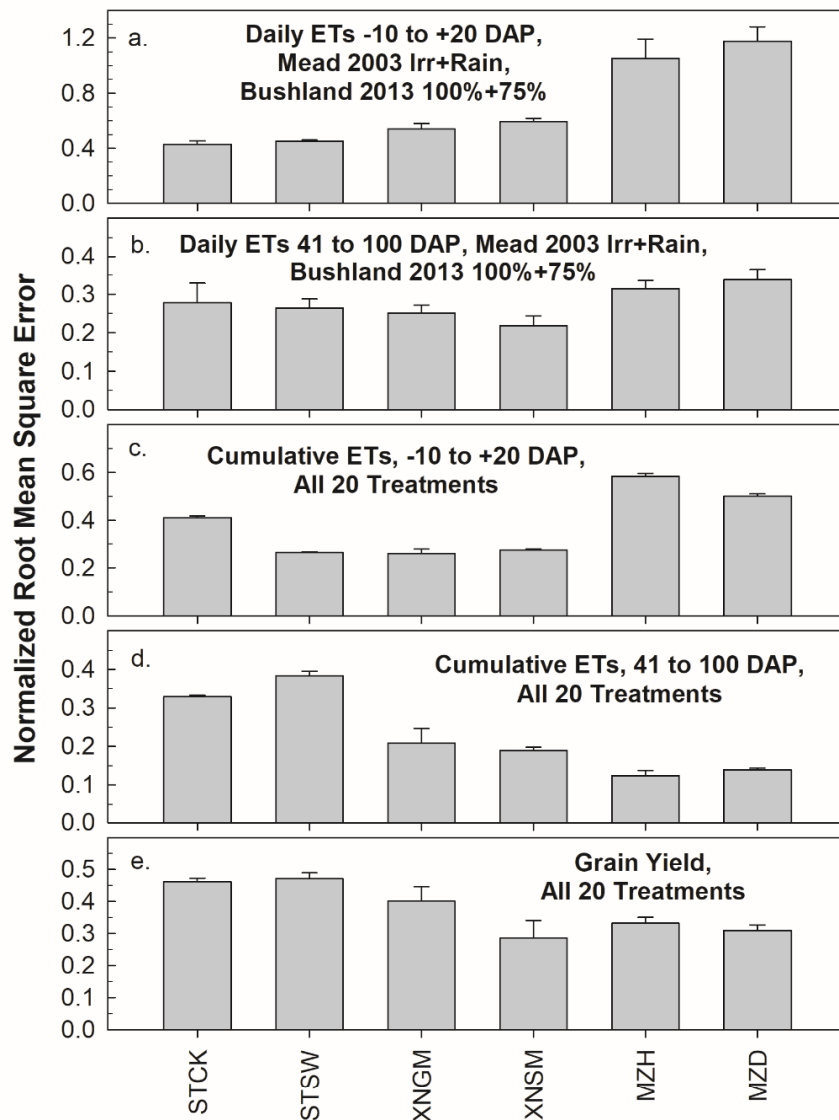


Figure 11. Direct comparisons using nRMSE between the STCK and STSW flavors of the STICS model family, between XNGM and XNSM flavors of Expert-N family, and between the MZH and MZD flavors of the MAZSIM model for (a) the -10 to +20 DAP time period (mostly soil E). The data used were all phases for the irrigated and rainfed data for Mead 2003 and the 100% and 75% MESA irrigated data for Bushland 2013. (b). Like (a) but for the 41 to 100 DAP period (mostly canopy T). (c.) Phase 4 of cumulative ETs from -10 to +20 DAP for all 20 treatments. (d) Like (c) but for cumulative ETs from 41 to 100 DAP. (e) Phase 4 grain yield for all 20 treatment-years.

ETs. Three of the models did not report  $ET_p$ , presumably the energy balance ones that do not use the concept.

Focusing on the Phase 2 results from irrigated Mead in 2003, 34 models reported  $E_p$  and 35 models reported  $T_p$ , and both  $E_p$  and  $T_p$  were quite variable (data not shown). As expected, the magnitude and variability of the soil  $E_p$  were greatest for bare soil at the beginning of the season. However, there was more than a 2 mm/day spread even at mid-season. Surprisingly, a few of the models showed some  $T_p$  starting on the day of planting before the plants had even emerged. Then, as the  $T_p$  increased in magnitude as plants grew to full size by mid-season, so did the range in variability among them, similar to ETs.

Thirteen of the models reported  $ET_o$  and only 4 reported  $ET_r$ . Presumably  $ET_o$  and  $ET_r$  depend only on weather, yet  $ET_o$  varied by a factor of about 2 at midseason among the 13 models (data not shown). Apparently, several different definitions and equations for  $ET_o$  are in play among these models.

Only 6, 4, 4, and 7 models used  $K_s$ ,  $K_{cb}$ ,  $K_e$ , and  $K_c$ , respectively. It seems likely that more models do use them, but they are computed and not routine output, so the modelers would have had to change code to get them. In any event, there appear to be several ways that models are getting from  $ET_o$  (or  $ET_r$ ) to  $ET_p$  that are contributing to the variability of ETs.

Thus, in conclusion, the variability in  $ET_p$  and ETs appears to be coming from steps all along the way starting from the calculations of  $ET_p$  to the final resultant ETs.

### 3.5 Cumulative month to whole season ETs results for all 20 treatment-years

The previous sections focused on the daily ET for four selected treatment-years. However, one can imagine that an underestimate of simulated daily ET one day could save some simulated soil moisture and lead to an overestimate the next day. The following sections examine the cumulative ET over longer time periods to reveal the extent that the errors are also cumulative.

#### 3.5.1 ETs from -10 to +20 DAP (mostly soil E) and 41 to 100 DAP (mostly canopy T)

Moving from daily ETs for the four cases (2003 for irrigated and rainfed Mead; 2013 MESA at 75% and 100% irrigation at Bushland) to cumulative ETs over longer time durations for all 20 treatment-years also showed wide variability among the models (Fig. 12). Again, there were variations by factors of 2 to more than 4 among them in cumulative ETs from -10 to +20 DAP (mostly soil E) (Fig. 12a). There was little or no improvement in going from Phase 1 to Phase 4. For Treatments 1-10 for Mead, the medians of the models were close to the observations, but for Treatments 11 and 12, the models generally overestimated ETs. For Bushland, most of the models underestimated Treatment 13 when spray irrigation wetted the surface and Treatment 18 when rainfall wetted the surface of SDI fields. Most models overestimated Treatments 17 and 19 when the SDI field surface was dry despite plentiful irrigation, but the medians were close to observed for the other 4 treatments. These results indicate problems simulating E from wetted surfaces and with simulated redistribution of water from buried drip lines to the surface (too much water movement to the surface).

Looking at cumulative ETs from 41 to 100 DAP (mostly canopy T), there is a range of about a factor of 2 among the models (Fig. 12b), which is bad but less than that from the bare soil (Fig.

12a). For Mead, most of the models overestimated ETs for Treatments 1-6 and 8-11. They underestimated Treatment 7 but were close for Treatment 12. For Bushland, most of the models underestimated ETs under sprinkler irrigation for Treatments 14-16, which represent wetter soil. Ranking the models' ability to simulate cumulative ETs from -10 to +20 DAP by nRMSE (Fig. 13a), the medians were close to observations for Phases 2-4. SLFT was the best model for Phases 2 and 3 and was next best in Phase 4. SLFT uses FAO-56 (Allen et al., 1998) to calculate atmospheric demand and then dual crop coefficients simulate ETs (Table S1). For Phase 2, models in the DSSAT family were ranked 3-7, and several did well in Phases 3 and 4. AMSW was best in Phase 4. CS and XNGM were among the best in Phases 3 and 4.

Similarly ranking their ability to simulate ETs from 41 to 100 DAP (Fig. 13b), several of the models in the DSSAT family did well for Phases 2, 3, and 4. ECOS was among the best for Phases 2 and 3. SSMi (which uses Priestly and Taylor (1972) for potential atmospheric demand and transpiration efficiency with biomass accumulation to simulate ETs) was ranked 6 for Phases 3 and 4, and SMET was ranked 3<sup>rd</sup> for Phase 4. surface conditions, but the medians were close for Treatment 13. Under SDI irrigation, most models underestimated Treatment 18, but the medians were close for Treatments 17, 19, and 20.



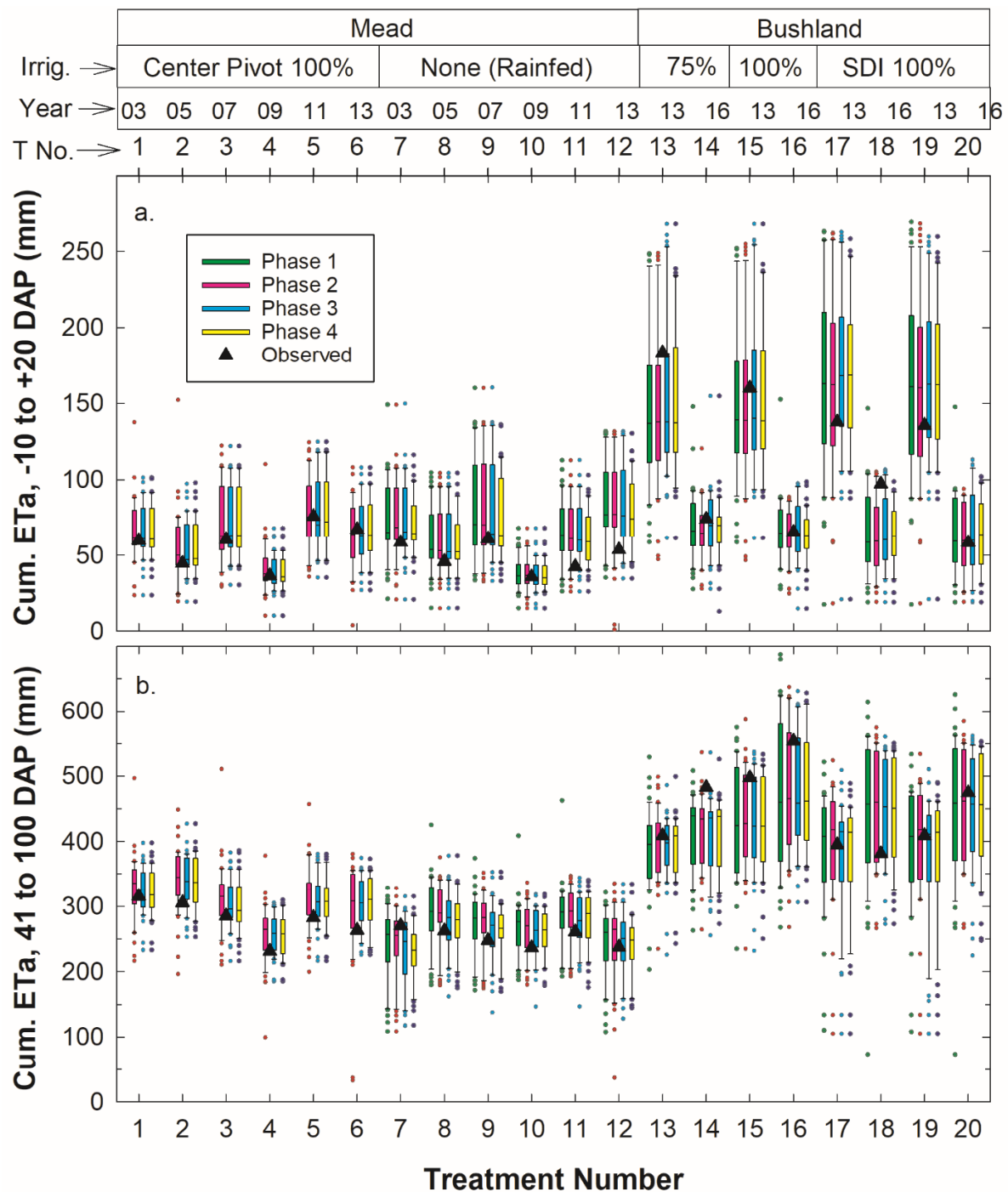


Figure 12. Box plots for all 20 treatment-years (as defined at the top) of cumulative simulated evapotranspiration (ETs) over (a) the -10 to +20 days after planting (DAP) time period (mostly E) and (b) the 41 to 100 DAP time period (mostly T) for all four phases. The dark lines across the boxes indicate the medians of all the models. Also shown are the corresponding observations. Phase 1 is not shown for treatments 1-6 because of a planting density mistake.

Looking back at Section 3.1.2.5, BIOM was among the best at simulating daily ETs, yet it was not among the best at simulating ETs over the longer intervals. On the other hand, DIFR was almost as good as BIOM for simulating daily ETs, and it was best for simulating cumulative ETs over the 41 to 100 DAP periods (Fig. 13, Phase 4). Besides DIFR, DCFS and SMET were the only other two models that were among the best for cumulative ETs over the 41 to 100 DAP periods and also were among the best for at least one case of daily ETs. For the -10 to +20 DAP periods, DCFR, XNGM and CS are the only models that were best for simulating cumulative ETs and also for daily ETs at least for one case. Thus, doing well for simulating daily ETs did not guarantee success at simulating cumulative ETs.

### 3.5.2 *Inter-comparisons of cumulative ETs within the DSSAT and other model families*

There were wide differences in performance among model “flavors” within the DSSAT family for cumulative simulated ETs from -10 to +20 DAP (mostly soil E) over the 20 treatment-years (Fig. 9c). Most obvious is that the Ritchie (1972) soil E method did much better than the corresponding Suleiman (Suleiman and Ritchie, 2003, 2004) method for every case. The Hydrus method did comparatively well for this cumulative-ETs/20-treatment-year comparison, which is in contrast to the daily-ETs/4-treatment-year comparison in Fig. 9a.

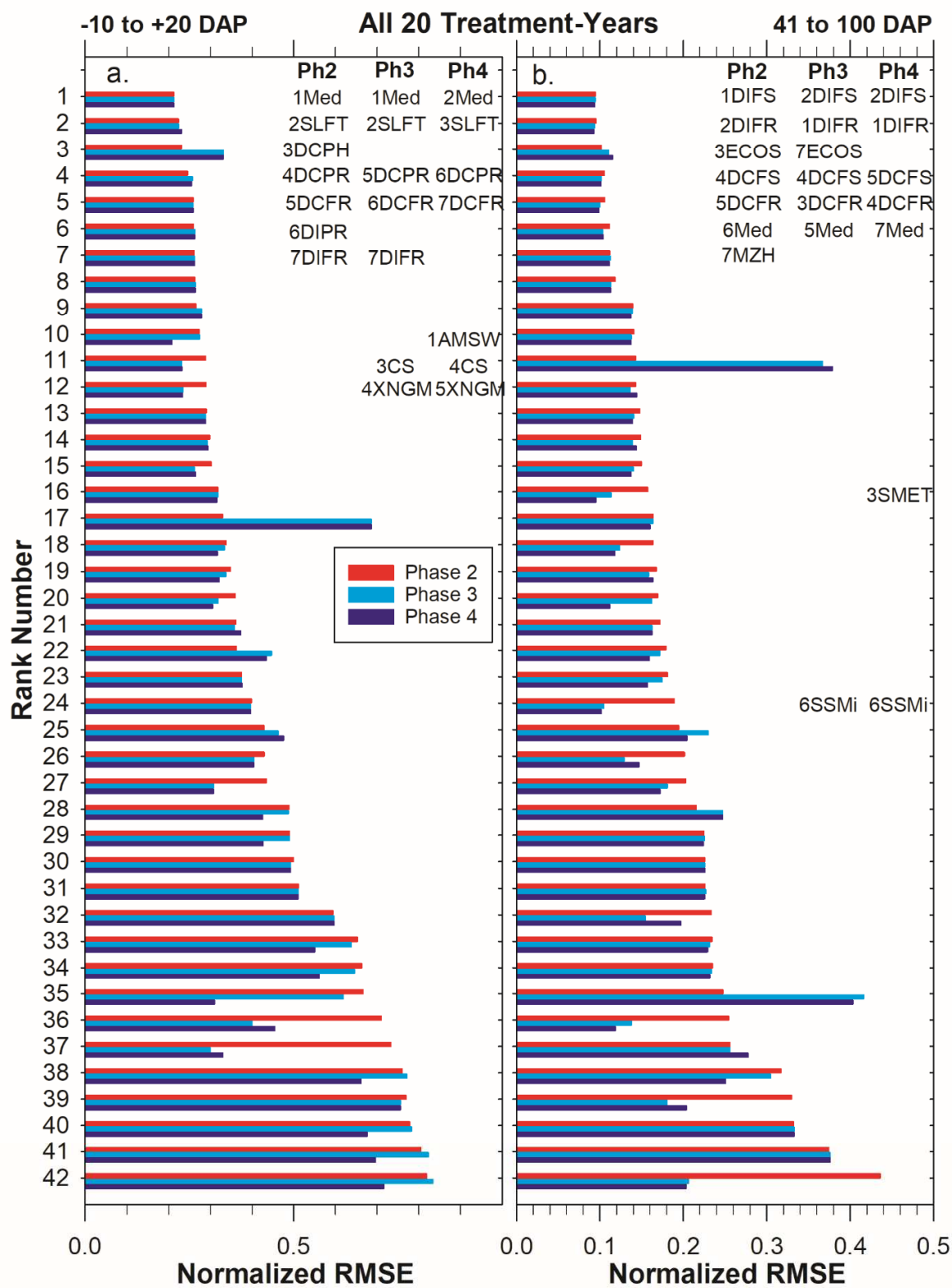


Figure 13. (a.) Normalized root mean squared error (nRMSE) between observed and simulated cumulative ET values from -10 to +20 days after planting (DAP)(mostly soil E) for all 20 treatment-years for all the models. Phases 2, 3, and 4 are identified by red, cyan, and blue bars with Phase 2 at the top and Phase 4 at the bottom of each group. The models have been sorted in ascending order of nRMSE for Phase 2 from top to bottom of the graph with the rank numbers on the left axis indicating their ranking for Phase 2. The Median (Med) and the six best models (lowest nRMSE) for Phase 2 are listed under “Ph2”. Somewhat similarly, the Median and six best models for Phases 3 and 4 are also listed under “Ph3”, and “Ph4”, but because the modelers made different adjustments going from phase to phase, their rank order changed, so the names along with their nRMSE rank are in different positions down the graph. Phase 1 is not shown because of the planting density error for the six irrigated Maize treatment-years. (b.) Same as for (a.) except the data are for 41 to 100 DAP (mostly crop canopy T).

As would be expected, looking at the 41 to 100 DAP periods, the soil E method had little effect (Fig. 9d). However, Hydrus, did poorly which is in contrast to the -10 to +20 periods (Fig. 9c).

There was no significant difference in performance between the CERES Maize and IXIM Maize models for the -10 to +20 DAP periods (Fig. 10c), whereas IXIM was slightly better than CERES for the 41 to 100 DAP periods (Fig. 10d). The better performance of IXIM for full canopy conditions was likely because of its more realistic simulation of LAI progression, as mentioned previously. Priestley-Taylor was the best ETp method for the -10 to +20 DAP periods (Fig. 10c) but worst for the 41 to 100 DAP periods (Fig. 10d). FAO-56 was second best for -10 to +20 DAP periods (Fig. 10c) but best for the 41 to 100 DAP periods (Fig. 10d). As was obvious from Fig. 9c, the direct comparison between Ritchie (1972) and Suleiman and Ritchie (2003) in Fig. 10c, confirms the superiority of the older Ritchie (1972) method for simulating soil E, likely because the Suleiman and Ritchie overestimates the upward movement of soil water from deeper depths. However, under full canopy conditions (Fig. 10d), there was no difference between the two soil E methods.

Looking at other models with more than one flavor, STSW performed better than STCK for cumulative ETs from -10 to +20 DAP (Fig. 11c), but the reverse was true from 41 to 100 DAP (Fig. 11d). It is somewhat surprising that the two-surface method for computing ETp in STSW did better for the -10 to +20 DAP period when there was only the single soil surface, but was worse for the 41 to 100 DAP full canopy period. However, looking more closely, both models did well for both time periods for the Mead data, whereas for Bushland in 2013, both models had trouble getting emergence with SDI in 2013, and this issue distorted the results. There was no

significant difference between XNGM and XNSM for either of the time periods (Figs. 11c, 11d). As noted in section 3.3, the two models use slightly different variants of the Penman-Monteith approach and differing root distribution approaches resulting in essentially no differences in daily ETs for the four cases (Figs 11a, 11b) nor in cumulative ETs for all 20 treatments (Figs. 11c, 11d). MZD did slightly better than MZH for the -10 to +20 DAP periods (Fig. 11c), but there was little difference for 41 to 100 DAP (Fig. 11d). Any differences between MZD and MZH are likely associated with the differences between interpolated and measured hourly weather data that were driving MZD and MZH, respectively.

*3.6 Ability of the models in Phase 4 to simulate agronomic parameters for all 20 treatment-years – maximum leaf area index, biomass at about 40 DAP and about 100 DAP, and final grain yield.*

#### *3.6.1 Considering all the models*

There was a wide range in simulations of maximum LAI between the lowest and the highest models (Fig. 14a). However, for some treatments, most of the models agreed closely as indicated by short boxes. Indeed, for Treatments 1 and 3, most of the models agreed almost exactly with one another and with observations. For many treatments, the medians agreed closely with observations. However, for Treatments 4 and 14, the models mostly underestimated LAI, whereas for Treatments 11, 15, and 17, they mostly overestimated LAI. For Bushland, treatments 15, 17, and 19 were in the 2013 year that began quite dry and required plentiful irrigation to achieve germination and to support crop growth. Overestimation of LAI may be linked to model algorithms overreacting to the plentiful irrigation in an otherwise stressful year.

Most of the models overestimated above-ground biomass at about 40 DAP for almost all the treatments (Fig. 14b). This was particularly true for the dry 2013 year at Bushland, again indicating that the plentiful irrigation caused the models to overestimate biomass accumulation despite an otherwise stressful environment. However, by 100 DAP (Fig. 14c), most of the models did much better, and agreement with observations was much closer. For final grain yield, most of the models did surprisingly well (Fig. 14d). For the irrigated Mead data (Treatments 1-6), most of the models agreed with one another and with the observations. They also did well for four of the Mead rainfed years, but underestimated Treatments 7 and 12. They did less well with the Bushland data, especially underestimating the SDI irrigation grain yields. The underestimation of SDI grain yields is likely tied to overly large partitioning of applied water to soil E, leaving less available water for T and grain yield formation. Many models, including DSSAT, lack true SDI capability and applied the water to the soil surface in this study. Because SDI was more efficient in water use than the MESA irrigation method in the actual fields used for this study (Evelt et al., 2020) and, therefore, likely will be more widely used in the future, the inability to handle SDI is an emerging lacuna in many of the models that should be addressed in future.

### 3.6.2 *Inter-comparisons of grain yield within the DSSAT and other model families*

DCFS was the best of the several model flavors within the DSSAT family to simulate grain yield, as indicated by nRMSE for Phase 4 (Fig. 9e). However, general patterns are not obvious in Fig. 9e. Nevertheless, some patterns emerge from a direct comparison in Fig. 10e. IXIM was slightly better than CERES. FAO-56 emerged as the best ET<sub>p</sub> method followed by Priestly-Taylor and then ASCE standardized reference ET equation with grass (short, 12 cm) crop

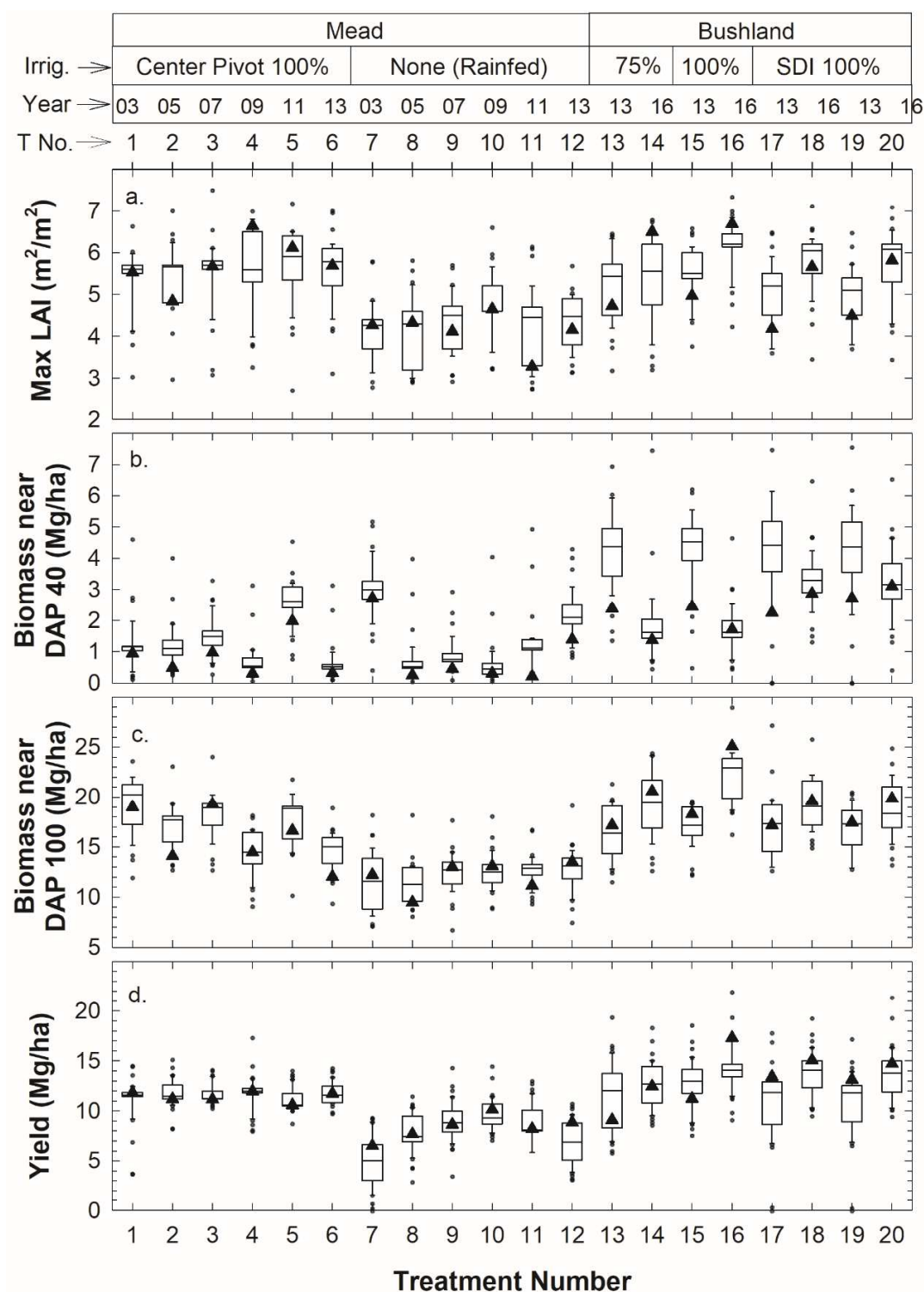


Figure 14. Box plots for Phase 4 of (a) maximum leaf area index, (b) biomass at about 40 days after planting (DAP), (c) biomass at about 100 DAP, and (d) final grain yield for all 20 treatment-years. Also shown are the corresponding observations (triangles).



coefficients and then alfalfa coefficients (tall, 50 cm) (Fig. 10e), which might be somewhat biased because they were not independently calibrated. There was no significant difference in the ability to simulate grain yield between the two methods for simulating soil E.

There was little difference in grain yield simulation ability between the two flavors of the STICS model or of the MAIZSIM model (Fig. 11e). However, XNSM tended to be better than XNGM, although XNGM uses a “more physiological” approach to simulate growth based on the principle of functional balance, in contrast to XNSM, in which a more or less predetermined scheme is used for partitioning of photosynthates.

### *3.7 K-means clusters*

In Figs. 15a and 15c the nRMSE of simulated grain yields for 40 of the models (plus their medians) and of simulated biomass accumulation for 39 of the models (plus their medians), respectively, are compared against the nRMSE of the simulated cumulative ETs for the -10 to +20 DAP time period (which was mostly Es for these mostly bare soil conditions). These graphs show that for many of the models the relative errors for simulating ETs tended to be larger than those for biomass and grain yield, which is consistent with the survey of Seidel et al. (2018) who found that few modelers calibrate the ET aspects of their models. Further, k-means clustering analyses with the number of clusters (k) specified to be four, the models were grouped into the four clusters illustrated in Figs. 15a and 15c. As can be seen, the k-means program identified a cluster of models that did quite well with the nRMSE for grain yields and biomass less than

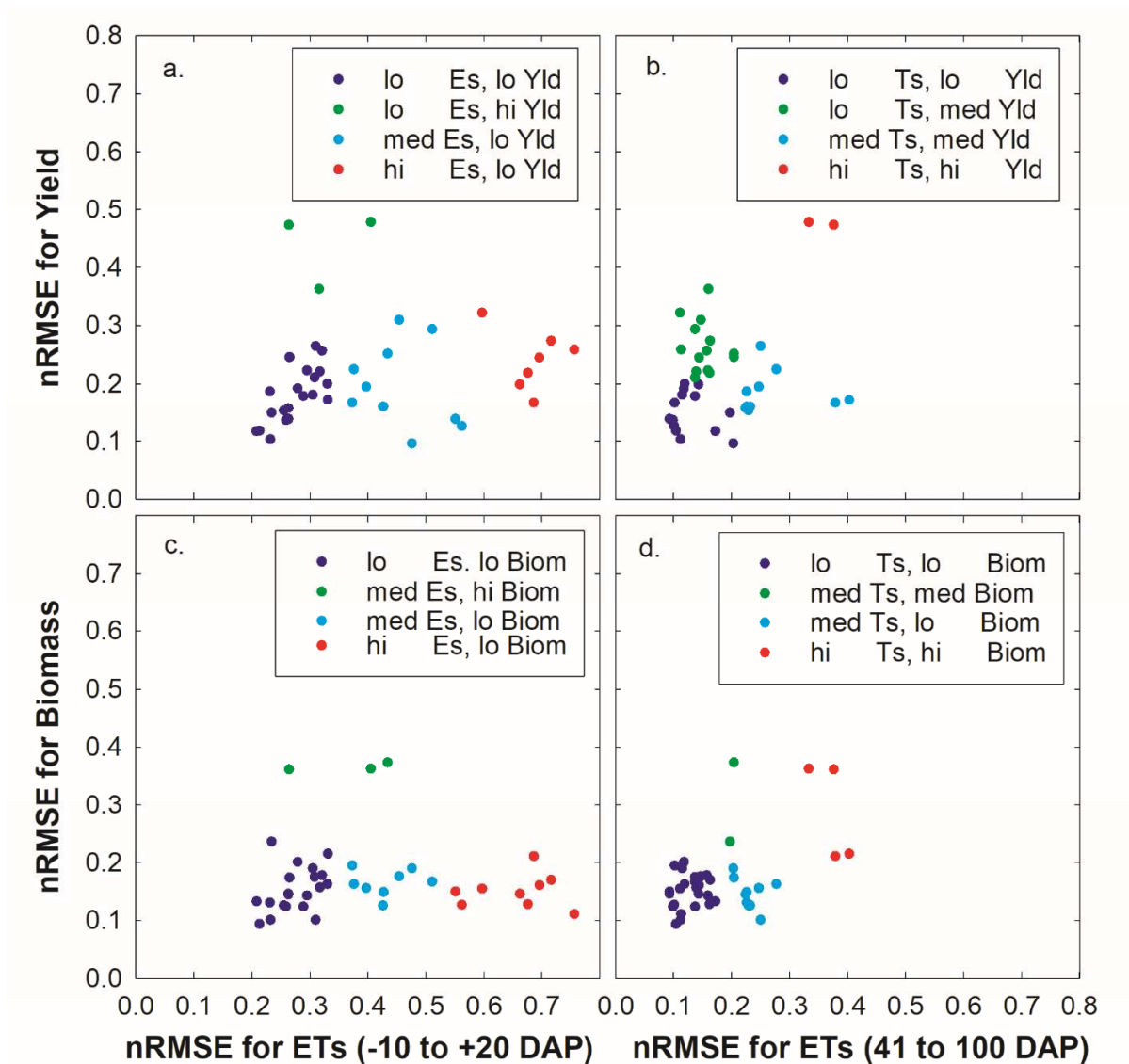


Figure 15. (a.) K-means clusters of the nRMSE for grain yields of 41 models (plus their median) for all 20 treatments versus the corresponding ETs for -10 to +20 DAP (mostly Ea). (b.) Same as (a) but for the 41 to 100 DAP periods (mostly Ta). (c.) K-means clusters of the nRMSE for biomass accumulation of 40 models (plus their median) from 41 to 100 DAP versus the corresponding ETs for from -10 to +20 DAP (mostly Ea). (d.) Same as (c) but for the 41 to 100 DAP periods (mostly Ts). (Note: one of the 41 models did not simulate grain yield and two did not simulate biomass.)

about 0.25 and that for ETs less than 0.35. One of the other clusters did poorly at simulating grain yield and biomass, and the other two clusters did progressively worse at simulating ETs. Figs. 15a and 15c suggest that a model's ability to simulate ETs well early in the growing season from -10 to +20 DAP can carry on through the seasons to help simulate biomass and grain yields well too.

Similarly, Figs. 15b and 15d illustrate the nRMSEs for grain yield and biomass against the nRMSE for the cumulative ETs from 41 to 100 DAP, when there were mostly full crop canopies. Comparing Fig. 15b with 15a and comparing Fig. 15d with 15c, it is apparent that the models were better at simulating the cumulative ETs for the full canopies than they were for bare soil at the beginning of the growing seasons. Again, k-means cluster analyses identified clusters of models that did quite well at simulating grain yields, biomass, and full canopy ETs quite well with the nRMSE of grain yield, biomass, and ETs all less than about 0.2. It is not surprising that there is such a cluster of models that can simulate ETs well during midseason which aids them to also simulate biomass and grain yields well.

Table 2 lists the models included in the best-performing clusters in Fig. 15. There is overlap among the four categories, but CS, AMSW, ECOS, XNSM, and AHC all excelled enough to appear in all four. Similarly performing well enough to appear in all four categories are three flavors from the DSSAT family: DIFR, DCFR, and DIGR. Not surprisingly, the ensemble median did very well, being first or second in all the categories, consistent with previous inter-comparisons, e.g., Asseng et al. (2015). Among these eight models, CS, XNSM, AHC, DIFR, DCFR, and DIGR all use FAO-56 (Allen et al., 1998) to compute ET<sub>p</sub> (Table S1). ET<sub>o</sub> was used

as E<sub>Tp</sub> for DIFR and DCFR, whereas DIGR used crop coefficients to adjust E<sub>To</sub> to E<sub>Tp</sub> and then various simulated or calculated crop or energy extinction coefficients were used to obtain E<sub>Ts</sub>. AMSW simulates T using the transpiration efficiency approach and E using Ritchie's (Ritchie, 1972) two-stage method (Probert et al., 1998; Keating et al., 2003). ECOS simulates E<sub>Ts</sub> from net radiation that is partitioned into latent, sensible, and soil heat fluxes with energy balances on the canopy and soil surfaces approach (Grant et al., 2007; Grant and Flanagan, 2007). DIGR uses the ASCE Standardized "Short Crop" (12-cm grass) E<sub>To</sub> (Allen et al., 2005), which is a successor to FAO-56, with maize crop coefficients computed from simulated LAI to adjust E<sub>To</sub> to E<sub>Tp</sub>. Thus, six of these models have similar core approaches for simulating E<sub>Ts</sub> but differ in other ways such as partitioning to leaf area or soil moisture movement, etc. AMSW and ECOS are both unique in their own ways within this elite group. The three DSSAT models all use the Ritchie-two-stage method for soil water evaporation rather than the Sulieman method, highlighting the need for E methods with improved upward movement of soil water and more accurate E loss in the incomplete canopy phase.

However, something all eight models have in common is that they all have been widely used for a long time under a wide range of conditions. This includes the lesser-known XNSM because it is a hybrid model with elements from both the CERES model (Jones and Kiniry, 1986) and the SUCROS model family (van Laar, 1992; Wang and Engel, 2000). AHC is also included because it was developed based on a coupling of the significantly modified SWAP model (van Dam et al., 1997) and the EPIC crop growth model (Williams et al., 1989). Thus, there has been time for several generations of modelers to improve these models so that they perform well over a wide range of climatic and soil conditions.

989

990 Table 2. Lists of models in Fig. 15 identified as being in the K-means clusters of best models  
 991 (lowest nRMSE) for Phase 4 for simulated grain yields and biomass versus lowest nRMSE for  
 992 simulated ETs for -10 to +20 DAP (mostly bare soil, Es) and 41 to 100 DAP (mostly closed  
 993 canopy, Ts). The models are ranked according to their sums of nRMSE for grain yield or  
 994 biomass plus that for ETs.

995

| Ranking | Yield vs. Es | Yield vs. Ts | Biomass vs Es | Biomass vs Ts |
|---------|--------------|--------------|---------------|---------------|
| 1       | AMSW         | Med          | CS            | Med           |
| 2       | Med          | CS           | Med           | CS            |
| 3       | CS           | AMSW         | DCFS          | DCFR          |
| 4       | XNGM         | SLFT         | DIFR          | SWB           |
| 5       | DCFR         | DCPR         | DIFS          | DCFS          |
| 6       | DIFR         | DCFR         | DCFR          | DIFR          |
| 7       | DCPR         | DIPR         | SSMi          | DIFS          |
| 8       | SLFT         | DIFR         | AMSW          | DIGR          |
| 9       | DIPR         | SLUS         | ECOS          | MZH           |
| 10      | DIGR         | DIGR         | DACT          | AHC           |
| 11      | XNSM         | DCGR         | XNSM          | DIGS          |
| 12      | ECOS         | BIOM         | DIGR          | DCGS          |
| 13      | DCPH         | XNGM         | AHC           | DIAR          |
| 14      | BIOM         | DIAR         | DIGS          | SSMi          |
| 15      | DCGR         | XNSM         | XNGM          | DCGR          |
| 16      | AQCP         | AQCP         |               | MZD           |
| 17      | AHC          | AHC          |               | AMSW          |
| 18      | DIAR         | ECOS         |               | ECOS          |
| 19      | SLUS         | DCAR         |               | DIAS          |
| 20      | DCAR         | DCRH         |               | AQCP          |
| 21      |              |              |               | XNSM          |
| 22      |              |              |               | TMOD          |
| 23      |              |              |               | DCAS          |
| 24      |              |              |               | DCAR          |

996

997

#### 4. Conclusions with discussion

4.1 Like the previous maize model ET inter-comparison (Kimball et al., 2019), again there was wide variability among the models in their ability to simulate ET, both on daily and on longer interval bases. The variability generally persisted even as the modelers received more information going from one phase to another, although a few modelers did make performance improvements.

4.2 Being among the best models at simulating daily ETs did not guarantee that a model would be among the best at simulating cumulative ETs.

4.3 Nevertheless, eight models, as well as the ensemble median, were identified that did well at simulating (a) cumulative ETs from -10 to +20 DAP (mostly soil E), (b) cumulative ETs from 40 to 100 DAP (mostly canopy T), (c) biomass accumulation, and (d) final grain yield. The models were CS, AMSW, ECOS, XNSM, AHC, DIFR, DCFR, and DIGR. Six of them follow the general approach of using FAO-56/Penman-Monteith (Allen et al., 1998, 2005) to simulate ETs, while AMSW uses a transpiration efficiency approach (Probert et al., 1998; Keating et al., 2003), and ECOS uses an energy balance approach (Grant et al., 2007; Grant and Flanagan, 2007). All of these models or their ancestors have been in existence and have been widely used for a long time. Thus, there has been time for improvement over a wide range of climatic and soil conditions. Unlike the previous inter-comparison (Kimball et al., 2019), none of the simpler models were among the best at simulating all four variables for this study involving a wider range of environmental conditions from two locations.

4.4 Although the ensemble median was not among the best estimates of soil moisture (Supplementary), it was at the top or close to the top for all other categories. That the

ensemble median generally outperforms any individual model is consistent with previous intercomparisons, e.g., Asseng et al. (2015).

4.5 Within the DSSAT family, the older Ritchie (1972) approach for simulating soil E was markedly better than the newer Suleiman and Ritchie (2003, 2004) approach, which appeared to overestimate upward movement of soil moisture.

4.6 Further, within the DSSAT family, the FAO-56 (Allen et al., 1998) method for calculating potential ET<sub>p</sub> was best for simulating ETs from 40 to 100 DAP (mostly canopy T) and worse for -10 to +20 DAP (mostly soil E). The Priestly and Taylor (1972) method was best for soil E and worse for canopy T. The ASCE Standardized Equation approach with short or tall crop coefficients (Allen et al., 2005) was intermediate for canopy T and worst for soil E, although this result might be somewhat biased because they were not independently calibrated.

4.7 DSSAT CSM-IXIM tended to be slightly better than DSSAT CSM-CERES for simulating canopy T, probably because IXIM simulated leaf area progression better.

4.8 Both STCK (which considers one surface to compute ET<sub>p</sub>) and STSW (which considers both soil and canopy surfaces to compute ET<sub>p</sub>) were among the best models to simulate ETs at the beginning of the seasons, with slightly better results for STSW. During the mid-season periods, STCK globally performed better than STSW, but both performed poorly with SDI in 2013, which distorted results.

4.9 XNSM and XNGM appeared to do equally well at simulating both soil E and canopy T, with XNGM following the more detailed Farquhar modeling approach in calculating photosynthesis and leafT, but greatly simplifying vertical root distribution. However,

1042 XNSM did better than XNGM at simulating grain yield, possibly due to its simpler but more  
1043 robust approach in simulating assimilate distribution among plant organs.

1044 4.9 MZD and MZH both have hourly time steps, yet MZD which uses daily weather data did  
1045 slightly better than MZH which uses hourly weather data at simulating soil E, but there was  
1046 no significant difference between them at simulating canopy T. This is somewhat surprising,  
1047 but nevertheless shows that simulated diurnal patterns of hourly weather can be as accurate  
1048 as using the actual hourly observations for input to crop growth models with hourly time  
1049 steps.

1050



1051

1052 **5 Acknowledgements**

1053 We appreciate access to the comprehensive dataset from Mead, Nebraska, USA, which was  
1054 collected by the following scientists: Shashi B. Verma, Achim Dobermann, Kenneth G.  
1055 Cassman, Daniel T. Walters, Johannes M. Knops, Timothy J. Arkebauer, George G. Burba,  
1056 Brigid Amos, Haishum Yang, Daniel Ginting, Kenneth G. Hubbard, Anatoly A. Gitelson, and  
1057 Elizabeth A. Walter-Shea. The dataset was collected with support from the DOE-Office of  
1058 Science (BER: Grant Nos. DE-FG03-00ER62996 and DE-FG02-03ER63639), DOE-EPSCoR  
1059 (Grant No. DE-FG02-00ER45827), and the Cooperative State Research, Education, and  
1060 Extension Service, US Department of Agriculture (Agreement No. 2001-38700-11092). Funding  
1061 was also provided by the National Multidisciplinary Laboratory for Climate Change, RRF-2.3.1-  
1062 21-2022-00014 project. Additional support was provided by grant "Advanced research  
1063 supporting the forestry and wood-processing sector's adaptation to global change and the 4th  
1064 industrial revolution", No. CZ.02.1.01/0.0/0.0/16\_019/0000803 financed by OP RDE. KW was  
1065 supported by the Met Office Hadley Centre Climate Programme funded by BEIS.

1066

1067 **6 Supplementary information**

1068 6.1 Word file with Table S1, which lists the ET simulation characteristics of the models plus  
1069 several figures showing an intercomparison among the models in their ability to simulate soil  
1070 moisture.

1071 6.2 Excel file with statistics and graphs showing the Phase 4 performance of the models in their  
1072 ability to simulate the daily ET observations for the irrigated and rainfed fields in Mead in  
1073 2003 and for the 100% and 75% MESA irrigated fields in Bushland in 2013. Also included

1074 are the statistics and graphs showing the models' ability to simulate cumulative ET from -10  
1075 to +20 DAP and from 41 to 100 DAP and agronomic parameters (maximum LAI, biomass at  
1076 about 100 DAP, and grain yields) for all 20 treatments.

1077

## References

- Allen, R. G., Pereira, L. S., Raes, D., Smith, M., 1998. *Crop Evapotranspiration: Guidelines for Computing Crop Water Requirements*, FAO Irrigation and Drainage Paper 56. Food and Agriculture Organization of the United Nations, Rome, Italy.
- Allen, R.G., Walter, I.A., Elliott, R., Howell, T., Itenfisu, D., Jensen, M., Snyder, R.L., 2005. The ASCE Standardized Reference Evapotranspiration Equation. American Society of Civil Engineers, Reston, Virginia. 195 pp.
- Asseng, S., Ewert, F., Rosenzweig, C., Jones, J.W., Hatfield, J.L, Ruane, A.C., Boote, K.J., Thorburn, P.J., Rötter, R.P., Cammarano, D., Brisson, N., Basso, B., Martre, P., Aggarwal, P.K., Angulo, C., Bertuzzi, P., Biernath, C., Challinor, A.J., Doltra, J., Gayler, S., Goldberg, R., Grant, R., Heng, L., Hooker, L., Hunt, L.A., Ingwersen, J., Izaurralde, R.C., Kersebaum, K.C., Müller, C., Naresh Kumar, S., Nendel, C., O'Leary, G., Olesen, J.E., Osborne, T.M., Palosuo, T., Priesack, E., Ripoche, D., Semenov, M.A., I. Shcherbak, I., Steduto, P., Stöckle, C., Stratonovitch, P., Streck, T., Supit, I., Tao, F., Travasso, M., Waha, M.K., Wallach, D., White, J.W., Williams, J.R., Wolf, J., 2013. Uncertainties in simulating wheat yields under climate change. *Nature Clim. Change* 3, 827-832.
- Asseng, S., Ewert, F., Martre, P., Rotter, R.P., Lobell, D.B., Cammarano, D., Kimball, B.A., Ottman, M.J., Wall, G.W., White, J.W., Reynolds, M.P., Alderman, P.D., Prasad, P.V.V., Aggarwal, P.K., Anothai, J., Basso, B., Biernath, C., Challinor, A.J., De Sanctis, G., Doltra, J., Fereres, E., Garcia-Vila, M., Gayler, S., Hoogenboom, G., Hunt, L.A., Izaurralde, R.C., Jabloun, M., Jones, C.D., Kersebaum, K.C., Koehler, A.K., Muller, C., Naresh Kumar, S., Nendel, C., O'Leary, G., Olesen, J.E., Palosuo, T., Priesack, E., Eyshi Rezaei, E., Ruane, A.C., Semenov, M.A., Shcherbak, I., Stockle, C., Stratonovitch, P., Streck, T., Supit, I., Tao, F., Thorburn, P.J., Waha, K., Wang, E., Wallach, D., Wolf, J., Zhao, Z., Zhu, Y., 2015. Rising temperatures reduce global wheat production. *Nature Clim. Change* 5, 143-147.
- Basso, B., Ritchie, J.T., 2015. Simulating crop growth and biogeochemical fluxes in response to land management using the SALUS model, in: Hamilton, S.K., Doll, J.E., G. P. Robertson, G.P. (Eds.), *The Ecology of Agricultural Landscapes: Long-Term Research on the Path to Sustainability*. Oxford University Press, New York, New York, USA. pp. 252-274.
- Bassu, S., Brisson, N., Durand, J-L., Boote, K., Lizaso, J., Jones, J.W., Rosenzweig, C., Ruane, A.C., Adam, M., Baron, C., Basso, B., Biernath, C., Boogaard, H., Conijn, S., Corbeels, M., Deryng, D., DeSanctis, G., Gayler, S., Grassini, P., Hatfield, J., Hoek, S., Izaurralde, C., Jongschaap, R., Kemanian, A.R., Kersebaum, K.C., Kim, S.-H., Kumar, N.S., Makowski, D., Mueller, C., Nendel, C., Priesack, E., Pravia, M.V., Sau, F., Shcherbak, I., Tao, F., Teixeira, E., Timlin, D., K. Waha, K., 2014. How do various maize crop models vary in their responses to climate change factors? *Global Change Biol.* 20, 2301-2320. doi: 10.1111/gcb.12520.

1119  
1120 Best, M.J., Pryor, M., Clark, D.B., Rooney, G.G., Essery, Ménard, C.B., Edwards, J.M., Hendry,  
1121 M.A., Porson, A., Gedney, A.N., Mercado, L.M., Sitch, S., Blyth, E., Boucher, O., Cox, P.M.,  
1122 Grimmond C.S.B., 2011. The Joint UK Land Environment Simulator (JULES), model  
1123 description Part 1: Energy and water fluxes. *Geoscientific Model Development*, Vol. 4, No. 3.  
1124 (01 September 2011), pp. 677-699, doi:10.5194/gmd-4-677-2011  
1125  
1126 Brisson, N., Perrier, A., 1991. A semi-empirical model of bare soil evaporation for crop  
1127 simulation models. *Water Resour. Res.* 27, 719-727.  
1128  
1129 Brisson, N., Itier, B., L'Hotel, J.C., Lorendeau J.Y., 1998. Parameterisation of the Shuttleworth-  
1130 Wallace model to estimate daily maximum transpiration for use in crop models. *Ecol. Model.*,  
1131 107, 159-169.  
1132  
1133 Brisson, N., Gary, C., Justes, E., Roche, R., Mary, B., Ripoche, D., Zimmer, D., Sierra, J.,  
1134 Bertuzzi, P., Burger, P., Bussière, F., Cabidoche, Y.M., Cellier, P., Debaeke, P., Gaudillère, J.P.,  
1135 Hénault, C., Maraux, F., Sequin, B., Sinoquet, H., 2003. An overview of crop model STICS. *Eur.*  
1136 *J. of Agron.*, 18, 309-332.  
1137  
1138 Cammarano, D., Rötter, R.P., Asseng, S., Ewert, F., Wallach, W., Martre, P., Hatfield, J.L.,  
1139 Jones, J.W., Rosenzweig, C., Ruane, A.C., Boote, K.J., Thorburn, P.J., Kersebaum, K.C.,  
1140 Aggarwal, P.K., Angulo, C., Basso, B., Bertuzzi, P., Biernath, C., Brisson, N., Challinor, A.J.,  
1141 Doltra, J., Gayler, S., Goldberg, R., Heng, L., Hooker, J.E., Hunt, L.A., Ingwersen, J.,  
1142 Izaurraldez, R.C., Müller, C., Kumar, S.N., Nendel, C., O'Leary, G., Olesen, J.E., Osborne,  
1143 T.M., Priesack, E., Ripoche, D., Steduto, P., Stöckle, C.O., Stratonovitch, P., Streck, T., Supit, I.,  
1144 Tao, F., Travasso, M., Waha, K., White, J.W., Wolf J., 2016. Uncertainty of wheat water use:  
1145 Simulated patterns and sensitivity to temperature and CO<sub>2</sub>. *Field Crops Res.*, 198, 80–92. doi:  
1146 [10.1016/j.fcr.2016.08.015](https://doi.org/10.1016/j.fcr.2016.08.015)  
1147  
1148 Constantin, J., Willaume, M., Murgue, C., Lacroix, B., Therond, O., 2015. The soil-crop models  
1149 STICS and AqYield predict yield and soil water content for irrigated crops equally well with  
1150 limited data. *Agric. For. Meteorol.*, 206, 55-68.  
1151  
1152 DeJonge, K. C., Thorp, K. R., 2017. Standardized reference evapotranspiration and dual crop  
1153 coefficient approach in the DSSAT Cropping System Model. *Trans. ASABE*, 60(6), 1965-1981.  
1154  
1155 Doorenbos, J., Pruitt. W.O., 1985. Guidelines for predicting crop water requirements. *FAO Irrig.*  
1156 *and Drain. Paper* 24. *FAO*, Rome.  
1157  
1158 Durand, J.L., Delusca, K., Boote, K.J., Lizaso, J., Manderscheid, R., Weigel, H.J., Ruane, A.C.,  
1159 Rosenzweig, C., Ahuja, L., Anapalli, S., Basso, B., Baron, C., Bertuzzi, P., Deryng, D., Ewert,

1160 F., Gaiser, T., Gayler, S., Heinlein, F., Kersebaum, F.C., Kim, S.H., Muller, C., Nendel, C.,  
 1161 Oliosio, A., Priesack, E., Villegas, J.R., Ripoche, D., Seidel, S.I., Srivastava, A., Tao, F., Timlin,  
 1162 D., Twine, T., Wang, E., Webber, H., Zhao, Z., 2018. How accurately do maize crop models  
 1163 simulate the interactions of atmospheric CO<sub>2</sub> concentration levels with limited water supply on  
 1164 water use and yield? *Eur. J. Agron.* (in press).  
 1165  
 1166 Evett, S.R., Heng, L.K., Moutonnet, P., Nguyen, M.L. (Eds.), 2008. Field estimation of soil  
 1167 water content: A practical guide to methods, instrumentation, and sensor technology. Vienna,  
 1168 Austria: International Atomic Energy Agency.  
 1169  
 1170 Evett, S.R., Kustas, W.P., Gowda, P.H., Anderson, M.C., Prueger, J.H., Howell, T.A., 2012.  
 1171 Overview of the Bushland evapotranspiration and agricultural remote sensing experiment 2008  
 1172 (BEAREX08): A field experiment evaluating methods for quantifying ET at multiple scales.  
 1173 *Advances in Water Resources* 50, 4-19. doi.org/10.1016/j.advwatres.2012.03.010  
 1174  
 1175 Evett, S.R., Marek, G.W., Colaizzi, P.D., Ruthardt, B.B., Copeland, K.S., 2018a. A subsurface  
 1176 drip irrigation system for weighing lysimetry. *Appl. Eng. Agric.*, 34(1), 213-221.  
 1177 <https://doi.org/10.13031/aea.12597>  
 1178  
 1179 Evett, S.R., Marek, G.W., Copeland, K S., Colaizzi, P D., 2018b. Quality management for  
 1180 research weather data: USDA-ARS, Bushland, TX. *Agrosystems, Geosciences, & Environment*  
 1181 1(1). <https://doi.org/10.2134/age2018.09.0036>  
 1182  
 1183 Evett, S.R., Marek, G.W., Colaizzi, P.D., Brauer, D.K., O'Shaughnessy, S.A., 2019. Corn and  
 1184 sorghum ET, E, yield, and CWP as affected by irrigation application method: SDI versus mid-  
 1185 elevation spray irrigation. *Transactions of the ASABE* 62(5), 1377-1393  
 1186 doi.org/10.13031/trans.13314.  
 1187  
 1188 Evett, S.R., Marek, G.W., Colaizzi, P.D., Brauer, D.K., Howell, T.A., 2020. Are crop  
 1189 coefficients for SDI different from those for sprinkler irrigation application? *Transactions of the*  
 1190 *ASAB*, 63(5), 1233-1242. doi.org/10.13031/trans.13920  
 1191  
 1192 Evett, S.R., Copeland, K.S., Ruthardt, B.B., Marek, G.W., Colaizzi, P.D., Howell, T.A., Sr.,  
 1193 Brauer, D.K., 2022. The Bushland, Texas Maize for Grain Datasets. *Ag Data*  
 1194 *Commons*. <https://doi.org/10.15482/USDA.ADC/1526317>  
 1195  
 1196 Fleisher, D.H., Condori, B., Quiroz, R., Alva, A., Asseng, S., Barreda, C., Bindi, M., Boote, K.J.,  
 1197 Ferrise, R., Franke, A.C., Govindakrishnan, P.M., Harahagazwe, D., Hoogenboom, G., Naresh  
 1198 Kumar, S., Merante, P., Nendel, C., Olesen, J.E., Parker, P.S., Raes, D., Raymundo, R., Ruane,  
 1199 A.C., Stockle, C., Supit, I., Vanuytrecht, E., Wolf, J., Woli, P., 2017. A potato model

intercomparison across varying climates and productivity levels. *Global Change Biol.* 23, 1258-1281.

Gauch, H.G., Hwang, J.T.G., Fick, G.W., 2003. Model evaluation by comparison of model-based predictions and measured values. *Agron. J.* 95, 1442-1446.

Goudriaan, J., 1977. Crop micrometeorology: A simulation study. Simulation monographs. PUDOC, Wageningen, the Netherlands.

Grant R.F., Arkebauer T.J., Dobermann A., Hubbard K.G., Schimelfenig T.T., Suyker A.E., Verma S.B., Walters, D.T., 2007. Net biome productivity of irrigated and rainfed maize – soybean rotations: modelling vs. measurements. *Agronomy Journal* 99, 1404-1423.

Grant, R. F., Flanagan, L.B., 2007. Modeling stomatal and nonstomatal effects of water deficits on CO<sub>2</sub> fixation in a semiarid grassland, *J. Geophys. Res.* 112, G03011, doi:10.1029/2006JG000302.

Hasegawa, T., Lai, T., Yin, X., Zhu, Y., Boote, K., Baker, J., Bregaglio, S., Buis, S., Confalonieri, R., Fugice, J., Fumoto, T., Gaydon, D., Naresh Kumar, S., Lafarge, T., Marcaida, M., Masutomi, Y., Nakagawa, H., Oriol, P., Ruget, F., Singh, U., Tang, L., Tao, F., Wakatsuki, H., Wallach, D., Wang, Y., Wilson, L.T., Yang, L., Yang, Y., Yoshida, H., Zhang, Z., Zhu, J., 2017. Causes of variation among rice models in yield response to CO<sub>2</sub> examined with Free-Air CO<sub>2</sub> Enrichment and growth chamber experiments. *Scientific Reports* | 7: 14858| DOI:10.1038/s41598-017-13582-y

Hidy, D., Barcza, Z., Marjanović, H., Ostrogović Sever, M. Z., Dobor, L., Gelybó, G., Fodor, N., Pintér, K., Churkina, G., Running, S., Thornton, P., Bellocchi, G., Haszpra, L., Horváth, F., Suyker, A., Nagy, Z., 2016. Terrestrial Ecosystem Process Model Biome-BGCMuSo v4.0: Summary of improvements and new modeling possibilities. *Geoscientific Model Development*, 9, 4405-4437. doi:10.5194/gmd-9-4405-2016

Hoogenboom, G., Porter, C.H., Boote, K.J., Shelia, V., Wilkens, P.W., Singh, U., White, J.W., Asseng, S., Lizaso, J.I., Moreno, L.P., Pavan, W., Ogoshi, R., Hunt, L.A., Tsuji, G.Y., Jones, J.W., 2019a. The DSSAT crop modeling ecosystem. In Boote, K. (ed.), *Advances in Crop Modelling for a Sustainable Agriculture*, Burleigh Dodds Science Publishing, Cambridge, UK, ISBN: 978 1 78676 240 5; www.bdspublishing.com)

Hoogenboom, G., Porter, C.H., Shelia, V., Boote, K.J., Singh, U., White, J.W., Hunt, L.A., Ogoshi, R., Lizaso, J.I., Koo, J., Asseng, S., Singles, A., Moreno, L.P., Jones, J.W., 2019b. Decision Support System for Agrotechnology Transfer (DSSAT) Version 4.7.

DSSAT Foundation, Prosser, Washington. <http://dssat.net>.

1241

1242 Jones, C.A., Kiniry, J.R., 1986. CERES-Maize: A Simulation Model of Maize Growth and  
 1243 Development. Texas A&M University Press, College Station, Texas. 194 pp.

1244

1245 Keating, B.A., Carberry, P.S., Hammer, G.L., Probert, M.E., Robertson, M.J., Holzworth, D.,  
 1246 Huth, N.I., Hargreaves, J.N.G., Meinke, H., Hochman, Z., McLean, G., Verburg, K., Snow, V.,  
 1247 Dimes, J.P., Silburn, M., Wang, E., Brown, S., Bristow, K.L., Asseng, S., Chapman, S.,  
 1248 McCown, R.L., Freebairn, D.M., Smith, C.J., 2003. An overview of APSIM, a model designed  
 1249 for farming system simulation. *Europ. J. Agron.*, 18, 267-288.

1250

1251 Kimball, B., Boote, K., Hatfield, J.L., Ahuja, L.R., Stockle, C., Archontoulis, S., Caron, C.,  
 1252 Basso, B., Bertuzzi, P., Constantin, J., Deryng, D., Dumont, B., Durand, J., Ewert, F., Gaiser, T.,  
 1253 Gayler, S., Hoffmann, M.P., Jiang, Q., Kim, S., Lizaso, J., Moulin, S., Nednel, C., Parker, P.,  
 1254 Palosuo, T., Priesack, E., Qi, Z., Srivastava, A., Tommaso, S., Tau, F., Thorp, K.R., Timlin, D.J.,  
 1255 Twine, T.E., Webber, H., Willaume, M., Williams, K., 2019. Simulation of maize  
 1256 evapotranspiration: An inter-comparison among 29 maize models. *Agricultural and Forest*  
 1257 *Meteorology*. 271:264-284.

1258

1259 Li, T., Hasegawa, T., Yin, X., Zhu, Y., Boote, K., Adam, M., Bregaglio, S., Buis, S.,  
 1260 Confalonieri, R., Fumoto, T., Gaydon, D., Marcaida III, M., Nakagawa, H., Oriol, P., Ruane,  
 1261 A.C., Ruget, F., Singh, B., Singh, U., Tang, L., Tao, F., Wilkens, P., Yoshida, H., Zhang Z.,  
 1262 Bouman, B., 2015. Uncertainties in predicting rice yield by current crop models under a wide  
 1263 range of climatic conditions. *Global Change Biol.* 21, 1328–1341.

1264

1265 Liu, B., Asseng, S., Müller, C., Ewert, F., Elliott, J., Lobell, D.P., Matre, P., Ruane, A.C.,  
 1266 Wallach, D., Jones, J.W., Rosenzweig, C., Aggarwal, P.K., Alderman, P.D., Anothai, J., Basso,  
 1267 B., Biernath, C., Cammarano, C.D., Challinor, A., Deryng, D., De Sanctis, G., Doltra, J., Fereres,  
 1268 E., Folberth, C., Garcia-Vila, M., Gayler, S., Hoogenboom, G., Hunt, L.A., Izaurralde, R.C.,  
 1269 Jabloun, M., Jones, C.D., Kersebaum, K.C., Kimball, B.A., A.-K. Koehler, A.-K., Kumar, S.N.,  
 1270 Nendel, C., O’Leary, G.J., Olesen, J.E., Ottman, M.J., Palosuo, T., Prasad, P.V.V., Priesack, E.,  
 1271 Pugh, T.A.M., Reynolds, M., Rezaei, E.E., Rötter, R.P., Schmid, E., Semenov, M.A., Shcherbak,  
 1272 Stehfest, I.E., Stöckle, C.O., Stratonovitch, P., Streck, T., Supit, I., Tao, F., Thorburn, P., Waha,  
 1273 K., Wall, G.W., Wang, E., White, J.W., Wolf, J., Zhao, Z., Zhu, Y., 2016. Similar estimates of  
 1274 temperature impacts on global wheat yield by three independent methods. *Nature Climate*  
 1275 *Change* 6, 1130-1138; DOI: 10.1038/NCLIMATE3115

1276

1277 Jones, J.W., Hoogenboom, G., Porter, C.H., Boote, K.J., Batchelor, W.D., Hunt, L.A., Wilkens,  
 1278 P.W., Singh, U., Gijsman, A.J., Ritchie, J.T., 2003. The DSSAT cropping system model.  
 1279 *European Journal of Agronomy* 18(3–4), 235–65. doi:10.1016/S1161-0301(02)00107-7.

1280

1281 Lopez-Cedron, F. X, Boote, K.J., Pineiro, J., Sau, F., 2008. Improving the CERES-Maize model  
 1282 ability to simulate water deficit effects on maize production and yield components. *Agron. J.*  
 1283 100, 296-307.  
 1284

1285 Maiorano, A., P. Martre, P., Asseng, S., Ewert, F., Müller, C., Rötter, R.P., Ruane, A.C.,  
 1286 Seminov, M.A., Wallach, D., Wang, E., Alderman, P.D., Kassie, B.T., Biernath, C., Basso, B.,  
 1287 Cammarano, D., Challinor, A.J., Doltra, J., Dumont, B., Rezaei, E.E., Gayler, S., Kersebaum,  
 1288 K.C., Kimball, B.A., Koehler, A.-K., Liu, B., O’Leary, G.J., Olesen, J.E., Ottman, M.J.,  
 1289 Priesach, E., Reynolds, M., Stratonovitch, P., Streck, T., Thorburn, P.J., Waha, K., Wall, G.W.,  
 1290 White, J.W., Zhao, Z., Zhu, Y., 2017. Crop model improvement reduces the uncertainty to  
 1291 temperature of multi-model ensembles. *Field Crops Res.*, 202, 5-20.  
 1292

1293 Masia, S., Trabucco, A., Spano, D., Snyder, R.L., Sušnik, J., Marras, S., 2021. A modelling  
 1294 platform for climate change impact on local and regional crop water requirements. *Agricultural*  
 1295 *Water Management* 255, 107005. DOI: 10.1016/j.agwat.2021.107005  
 1296

1297 Mancosu, N., Spano, D., Orang, M., Sarreshteh, S., Snyder R.L., 2016. SIMETAW#—a model  
 1298 for agricultural water demand planning. *Water Resources Management*: 30, 541-557.  
 1299 DOI:10.1007/s11269-015-1176-7.  
 1300

1301 Marek, T.H., Schneider, A.D., Howell, T.A., Ebeling, L.L., 1988. Design and construction of  
 1302 large weighing monolithic lysimeters. *Trans. ASAE*, 31(2), 477-484.  
 1303 doi.org/10.13031/2013.30734  
 1304

1305 Marek, G.W., Evett, S.R., Gowda, P.H., Howell, T.A., Copeland, K.S., Baumhardt, R.L., 2014.  
 1306 Post-processing techniques for reducing errors in weighing lysimeter evapotranspiration (ET)  
 1307 datasets. *Trans. ASABE* 57(2), 499-515. <https://dx.doi.org/10.13031/trans.57.10433>  
 1308

1309 Monteith, J.L., 1965. Evaporation and environment. 19<sup>th</sup> Symposia of the Society for  
 1310 Experimental Biology, University Press, Cambridge, 19, 205-234.  
 1311

1312 Moore, C., Berardi, D., Blanc-Betes, E., DeLucia, E.H., Dracup, E.C., Egenriether, S., Gomez-  
 1313 Casanovas, S.N., Hartman, M.D., Hudiburg, T., Kantola, I., Masters, M.D., Parton, W.J., van  
 1314 Allen, R., von Haden, A.C., Wang, W.H., and Bernacchi, C.J., 2020. The carbon and nitrogen  
 1315 cycle impacts of reverting perennial bioenergy switchgrass to an annual maize crop rotation.  
 1316 *GCB Bioenergy*, 12:941-954. (<http://dx.doi.org/10.1111/gcbb.12743>).  
 1317  
 1318

1319 Pedregosa, F., Varoquaux, G., Gramfort, A., Michel, V., Thirion, B., Grisel, O., Blondel, M,  
 1320 Prettenhofer, P., Weiss, R., Dubourg, V., Vanderplas, J., Passos, A., Cournapeau, D., Brucher,



1321 M., Perrot, M., Duchesnay, E., 2011. Scikit-learn: Machine learning in Python. *Journal of*  
 1322 *Machine Learning Research* 12, 2825-2830.

1323

1324 Perego, A., Giussani, A., Sanna, M., Fumagalli, M., Carozzi, M., Alfieri, L., Brenna,  
 1325 S., Acutis, M., 2013. The ARMOSA simulation crop model: overall features,  
 1326 calibration and validation results. *Ital. J. Agrometeorology* 3, 23–38.

1327

1328 Penman, H.L., 1948. Natural evaporation from open water, bare soil, and grass. *Proc. Royal Soc.*  
 1329 *London*, 194, 120-145.

1330

1331 Priesack, E., Gayler, S., Hartmann, H.P., 2006. The impact of crop growth sub-model choice on  
 1332 simulated water and nitrogen balances. *Nutrient Cycling in Agroecosystems* 75, 1-13. DOI  
 1333 10.1007/s10705-006-9006-1.

1334

1335 Priestley, C.H.B., Taylor, R.J., 1972. On the assessment of surface heat flux and evaporation  
 1336 using large-scale parameters. *Monthly Weather Rev.* 100, 81-92.

1337

1338 Probert, M.E.E., Dimes, J.P.P., Keating, B.A.A., Dalal, R.C.C., Strong, W.M.M., 1998.  
 1339 APSIM's water and nitrogen modules and simulation of the dynamics of water and nitrogen in  
 1340 fallow systems. *Agric. Syst.* 56, 1–28. doi:10.1016/S0308-521X(97)00028-0.

1341

1342 Ritchie, J.T., 1972. Model for predicting evaporation from a row crop with incomplete cover.  
 1343 *Water Resour. Res.* 8, 1204-1213.

1344

1345 Sau, F., Boote, K.J., Bostick, W.M., Jones, J.W., Minguez, M.I., 2004. Testing and improving  
 1346 evapotranspiration and soil water balance of the DSSAT crop models. *Agron. J.* 96, 1243-1257.

1347

1348 Seidel, S.J., Palosuo, T., Thorburn, P., Wallach, D., 2018. Towards improved calibration of models –  
 1349 Where are we now and where should we go? *European J. Agron.* 94, 25-35.  
 1350 doi.org/10.1016/j.eja.2018.01.006

1351

1352 Shelia, V., Šimůnek, J., K.J. Boote, K.J., Hoogenboom. G., 2018. Coupling DSSAT and  
 1353 HYDRUS-1D for simulations of soil water dynamics in the soil-plant-atmosphere system.  
 1354 *Journal of Hydrology and Hydromechanics* 66(2), 232-245.

1355

1356 Shuttleworth, W.J., Wallace, J.S., 1985. Evaporation from sparse crops - an energy combination  
 1357 theory. *Quart. J. Roy. Meteorol. Soc.* 111, 839-855.

1358

1359 Šimůnek, J., Huang, K., van Genuchten, M., 1998. The HYDRUS code for simulating the one-  
 1360 dimensional movement of water, heat, and multiple solutes in variably-saturated media, version

6.0., Tech. Rep. 144, U.S. Salinity Lab., United States Dep. of Agriculture, Agricultural Research Service.

Šimůnek, J., van Genuchten, M. T., Šejna, M. 2008. Development and Applications of the HYDRUS and STANMOD Software Packages and Related Codes. *Vadose Zone Journal*, 7(2), 587. <https://doi.org/10.2136/vzj2007.0077>

Soltani, A., Sinclair, T.R., 2012. *Modeling Physiology of Crop Development, Growth and Yield*, CABI International (2012), 322 pp.

Stöckle, C.O., Donatelli, M., Nelson, R., 2003. CropSyst, a cropping systems simulation model. *Eur. J. Agron.* 18, 289–307.

Suleiman, A.A., Ritchie, J.T., 2003. Modeling soil water redistribution during second-stage evaporation. *Soil Sci. Soc. Amer. J.*, 67, 377-386.

Suleiman, A.A., Ritchie, J.T., 2004. Modifications to the DSSAT Vertical Drainage Model for more accurate soil water dynamics estimation. *Soil Science*, 169,745-757. DOI 10.1097/01.ss.0000148740.90616.fd

Suyker, A.E., Verma, S.B., Burba, G.G., Arkebauer, T.J., Walters, D.T., Hubbard, K.G., 2004. Growing season carbon dioxide exchange in irrigated and rainfed maize. *Agricultural and Forest Meteorology* 124, 1-13.

Suyker, A.E., Verma, S.B., Burba, G.G., Arkebauer, T.J., 2005. Gross primary production and ecosystem respiration of irrigated maize and irrigated soybean during a growing season. *Agricultural and Forest Meteorology* 131, 180-190.

Suyker, A.E., Verma, S.B., 2008. Interannual water vapor and energy exchange in an irrigated maize-based agroecosystem. *Agricultural and Forest Meteorology* 148, 417-427.

Suyker, A.E., Verma, S.B., 2009. Evapotranspiration of irrigated and rainfed maize-soybean cropping systems. *Agricultural and Forest Meteorology* 149, 443-452.

Thorp, K.R., Marek, G.W., DeJonge, K.C., Evett, S.R., 2020. Comparison of evapotranspiration methods in the DSSAT Cropping System Model: II. Algorithm performance. *Computers and Electronics in Agriculture* 177, 105679.

van Dam, J.C., Huygen, J., Wesseling, J.G., Feddes, R.A., Kabat, P., van Walsum, P.E.V. et al., 1997. *Theory of SWAP Version 2.0. Simulation of Water Flow, Solute Transport and Plant*

- Growth in the Soil–Water–Atmosphere–Plant Environment, Department of water resources, WAU, Report 71, technical Document 45, DLO Winand Staring Centre-DLO.
- van Laar, H.H., Goudriaan, J., and van Keulen, H. (eds), 1992. Simulation of crop growth for potential and water-limited production situations (as applied to spring wheat). Simulation Reports CABO-TT, no. 27, Wageningen, 72 pp.
- Villalobos, F.J., Fereres. E., 1990. Evaporation measurements beneath corn, cotton, and sunflower canopies. *Agron. J.* 82, 1152-1159.
- Wang, E. and Engel, T., 2000. SPASS: a generic process-oriented crop model with versatile windows interfaces. *Environmental Modelling & Software* 15, 179-188.
- Wang, E., Martre, P., Ewert, F., Zhao, Z., Maiorano, A., Rötter, R.P., Kimball, B.A, Ottman, M.J., Wall, G.W, White, J.W, Reynolds, M.P., Alderman, P.D., Aggarwal, P.K., Anothai, J., Basso, B., Biernath, Cammarano, D., Challinor, A.J., De Sanctis, G., Doltra, J., Fereres, E., Garcia-Vila, M., Gayler, S., Hoogenboom, G., Hunt, L.A., Izaurrealde, R.C., Jabloun, M., Jones, C.D., Kersebaum, K.C., Koehler, A.-K., Müller, C., Liu, L., Kumar, S.N., Nendel, C., O’Leary, G., Olesen, J.E., Palosuo, T., Priesack, E., Rezaei, E.E., Ripoche, D., Ruane, A.C., Semenov, M.A., Shcherbak, I., Stöckle, C., Stratonovitch, P., Streck, T., Supit, I., Tao, F., Thorburn, P., Waha, K., Wallach, D., Wang, Z., Wolf, J., Zhu, Y., Asseng, S., 2017. The uncertainty of crop yield projections is reduced by improved temperature response functions. *Nature Plants* 3 (1702), 1-11. DOI: 10.1038/nplants.2017.102
- Williams, J.R., Jones, C.A., Kiniry, J.R., and Spanel, D.A., 1989. The EPIC crop growth model. *Transactions of the ASAE* 32(2), 497-511.
- Willmott, C.J. 1982. Some comments on the evaluation of model performance. *Bulletin American Meteorological Society* 63(11), 1309-1313.
- Wolf, J., 2012. User Guide for LINTUL5: Simple Generic Model for Simulation of Crop Growth under Potential, Water Limited and Nitrogen, Phosphorus and Potassium Limited Conditions. Wageningen University.
- Yang, Y., Kim, S-H, Timlin, D. J., Fleisher, D.H, Quebedeaux, B., Reddy, V. R., 2009. Simulating canopy evapotranspiration and photosynthesis of corn plants under different water status using a coupled MaizeSim+2DSOIL Model. *Trans. ASAE*, 52(3), 1011-1024.